

11 Polar Quantum Criticality: Challenges and Opportunities

Premala Chandra

Rutgers University

136 Frelinghuysen Road, Piscataway NJ 08854, USA

Contents

| | | |
|----------|--|-----------|
| 1 | Quantum criticality and polar materials? | 2 |
| 1.1 | Quantum criticality primer | 2 |
| 1.2 | Polar quantum criticality? | 8 |
| 2 | Quantum annealed criticality | 11 |
| 2.1 | The challenge: classical first-order transitions! | 11 |
| 2.2 | Adaptation of the Larkin-Pikin approach | 12 |
| 2.3 | Quantum annealing of the first-order transition | 18 |
| 3 | Novel metallicity | 22 |
| 3.1 | The challenge: how to couple electrons to a soft polar mode? | 22 |
| 3.2 | Spin-orbit assisted electron-phonon interactions | 23 |
| 3.3 | Multiband strongly correlated electronic phases | 24 |
| 4 | Unconventional superconductivity (with only phonons!) | 27 |
| 4.1 | The challenge: anti-adiabatic and isotropic! | 27 |
| 4.2 | Historical context | 27 |
| 4.3 | Superconductivity with transverse phonons | 28 |
| 4.4 | Comparison with experiment . . . and homework! | 30 |
| 5 | Summary and outlook | 32 |

1 Quantum criticality and polar materials?

Intuitively the link between polar materials and quantum criticality is not at all obvious. Polar materials are mostly insulators with discontinuous classical transitions, whereas quantum criticality is often studied in itinerant magnetic systems towards the characterization of novel metallic behaviors. Nonetheless I hope to convince you that there is much to be gained at the confluence of these two research areas. After unpacking the title, I will present a theoretical basis for how the interplay of classical first-order transitions with quantum fluctuations can restore quantum criticality in compressible insulators. Next we will turn to strongly correlated phases in quantum critical polar metals, including non-Fermi liquids. The miracle and the mystery of unconventional superconductivity in the nearly quantum critical system n-doped SrTiO₃ will be our last topic. We will end with a summary and outlook for future work.

In the course of our discussion, I will make an effort to present a more expansive treatment of topics that may not be in the mainstream lexicon; these include simple ways to determine the temperature-dependence of observables near quantum critical points, crossover scaling for when both quantum and classical critical fluctuations are present, and subtleties involving $q = 0$ and $q \neq 0$ elastic degrees of freedom. Naturally I will be sharing with you a very personal perspective, and I will do my best to provide references whenever appropriate to provide more details and to broaden the viewpoints expressed here for the curious reader.

1.1 Quantum criticality primer

At classical phase transitions, thermal fluctuations melt the long-range order. By contrast quantum criticality, associated with continuous quantum phase transitions, occurs at zero temperature where thermal fluctuations are absent; here the phase change is driven by zero-point fluctuations whose magnitude can be tuned by pressure or field. My aim here is to present the key ideas of quantum criticality with minimal formalism, using familiar concepts whenever possible; there are several excellent resources for readers eager for more specifics [1–5]. My emphasis will be on determining the temperature-dependence of observable quantities near quantum critical points, and our discussion here will follow closely an approach that three experimental colleagues (G.G. Lonzarich, S.E. Rowley and J.F. Scott) and I have developed together [6].

Aren't quantum fluctuations only present at zero temperature? According to the Heisenberg uncertainty principle, temporal uncertainty is inversely proportional to that in the energy

$$\Delta t \propto \hbar/\Delta E \quad \Rightarrow \quad \tau_P \propto \hbar/k_B T \quad (1)$$

so that the decoherence timescale, the Planck time τ_P , of the quantum fluctuations, is inversely proportional to the temperature. Fluctuations are purely quantum up to τ_P , and are classical beyond it. At a $T = 0$ quantum critical point, τ_P is infinite so the fluctuations are purely quantum. The Planck time-scale decreases with increasing temperatures and quantum fluctuations remain important roughly up to the Debye temperature, determined by phonon frequencies, that can be several hundred Kelvin. Thus, unlike its classical counterpart, the quantum critical region

can have significant presence in a temperature-pressure phase diagram indicating the important influence of the zero-temperature critical point. From another perspective, quantum fluctuations are important for temperatures bounded by the condition

$$\hbar\omega \sim k_B T \quad (\omega \propto q^z) \quad \Rightarrow \quad \xi_Q \propto (\tau_P)^{1/z} \quad \text{and} \quad q_T \propto T^{\frac{1}{z}} \quad (2)$$

which, combined with the dispersion ($\omega \propto q^z$), leads to a corresponding quantum correlation length ξ_Q where z is the dynamical exponent; fluctuations are classical on length-scales greater than ξ_Q with a corresponding thermal momentum cutoff q_T for thermally activated modes. Therefore, for temperatures where ξ_Q is greater than the lattice spacing, the thermal correlation volume contains a quantum mechanical core on length-scales and time-scales determined by ξ_Q and τ_P ; in momentum space the thermal wavevector q_T is a cutoff for classical fluctuations when their quantum counterparts are present [6], as we shall discuss shortly.

What defines the quantum critical region? It is crucial to note that temperature is *not* a simple tuning parameter at a quantum phase transition. Indeed T provides the low-energy cutoff for quantum fluctuations through the Planck time-scale τ_P so that temperature plays the role of a finite-size effect in time at a quantum critical point [4, 7]. The quantum critical region is defined by the interplay between the scale-invariant order parameter fluctuations and the temporal boundary conditions imposed by finite temperature; here a system's thermodynamic behavior depends on both space and time, observable experimentally with signatures distinct from its classical counterpart.

Can one see the coexistence of quantum and classical fluctuations in a simple example?

Let us illustrate these concepts by considering the amplitude fluctuations of a one-dimensional harmonic oscillator (1d SHO) as a function of temperature whose variance is

$$\langle x^2 \rangle = \frac{\Omega}{\mathcal{K}} \left(n_\Omega + \frac{1}{2} \right) \quad (3)$$

where $n_\Omega = 1/(\exp(\Omega/T) - 1)$ is the Bose factor and we have set the constants $\hbar = k_B = 1$ (see Fig. 1). Here the important energy scales are the temperature T and the oscillator frequency Ω . If $T \gg \Omega$, then $n_\Omega \sim T/\Omega$ and the variance $\langle x^2 \rangle$ scales with T and Ω drops out completely. In this instance, the total variance results from purely classical (thermal) fluctuations. However for lower temperatures, specifically in the interval $0 \leq T \leq \Omega$, there is another contribution to $\langle x^2 \rangle$ due to quantum fluctuations. The total variance then becomes the sum of the quantum and classical components, where at $T = 0$ only the quantum component survives.

What does the behavior of a 1d SHO have to do with quantum phase transitions?

Let me explain the conceptual connection. Order parameter fluctuations play an important role at phase transitions, and we can consider the variance of each of their Fourier components one at a time. Let us call each of these Fourier components a mode of wavevector q whose behavior can be mapped onto that of a simple harmonic oscillator of amplitude x with oscillator frequency Ω . At a continuous transition, the mode stiffness \mathcal{K} vanishes for modes close to the ordering wavevector and the amplitude fluctuations diverge. If this occurs at $T \gg \Omega$, then the transition may be driven by essentially classical fluctuations. However at lower temperatures

Simple Harmonic Oscillator

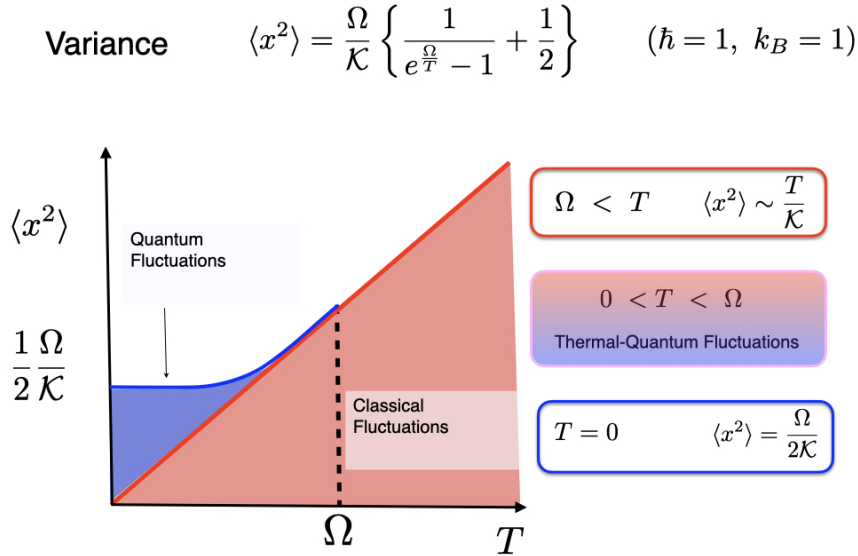


Fig. 1: Amplitude of a simple harmonic oscillator with frequency Ω and stiffness \mathcal{K} as a function of temperature.

where $0 \leq T \leq \Omega$, both classical and quantum fluctuations are present and these “hybrid” fluctuations lead to behaviors and orderings distinct from those driven solely by their classical counterparts. Again \mathcal{K} is zero at the ordering wavevector but now there are both quantum and classical contributions to $\langle x^2 \rangle$. Of course at strictly $T = 0$ the fluctuations are purely quantum.

Why is “ $d+z$ ” the effective dimension of a quantum critical system? Since for purely classical fluctuations, the amplitude of each mode of wavevector q depends only on the temperature, its statistical mechanical description involves d spatial dimensions. However when quantum fluctuations are present, both the mode frequency and T are important. More generally each mode has a power spectrum of frequencies that results in a statistical mechanical description involving the summation over both the wavevectors and the frequency. The number of dimensions associated with the dynamics is associated with the frequency-wavevector dispersion relation; then the overall effective dimensionality will be $D = d+z$, referring to d space and z time dimensions, where z is the dynamical exponent associated with the dispersion of the mode frequency.

Our focus here is on the temperature-behavior of observable quantities near a quantum critical point. Towards this goal, let us resume our discussion of order parameter fluctuations where we treated each Fourier mode as a simple harmonic oscillator of amplitude x with frequency Ω . The total variance in the mode amplitude is then

$$\langle x^2 \rangle = \left(n_\Omega + \frac{1}{2} \right) \Omega \chi \quad (4)$$

where n_ω refers to the Bose function and $\chi = \frac{1}{\mathcal{K}} = \text{Re } \chi_{\omega=0}$ where \mathcal{K} is the stiffness. We recall that for a simple harmonic oscillator

$$\text{Im } \chi_\omega = \frac{\pi}{2} \omega \chi \delta(\omega - \Omega) \quad (\omega > 0) \quad (5)$$

so that we can rewrite (4) as

$$\langle x^2 \rangle = \frac{2}{\pi} \int_0^\infty d\omega \left(n_\omega + \frac{1}{2} \right) \text{Im} \chi_\omega. \quad (6)$$

We note that this link between the variance of amplitude fluctuations and the imaginary part of the response, here derived for a simple harmonic oscillator, is actually a much more general result associated with the fluctuation dissipation (Nyquist) theorem [8].

We can generalize (6) to a sum of all wavevector q modes, for example, over the entire Brillouin zone. In anticipation of our discussion of polar quantum criticality, let us now transition to the amplitude of the scalar order parameter ϕ that is an electric dipole moment density. Then, following our previous line of reasoning, the variance of the amplitude fluctuations of the moment is

$$\langle \delta\phi^2 \rangle = \frac{2}{\pi} \sum_q \int_0^\infty d\omega \left(n_\omega + \frac{1}{2} \right) \text{Im} \chi_\omega = \langle \delta\phi_T^2 \rangle + \langle \delta\phi_{ZP}^2 \rangle \quad (7)$$

where $\phi = \bar{\phi} + \delta\phi$, $\bar{\phi}$ is the average, $\langle \delta\phi \rangle = 0$ and

$$\text{Im} \chi_{q\omega} = \frac{\pi}{2} \omega_q \chi \delta(\omega - \omega_q) \quad (\omega > 0) \quad (8)$$

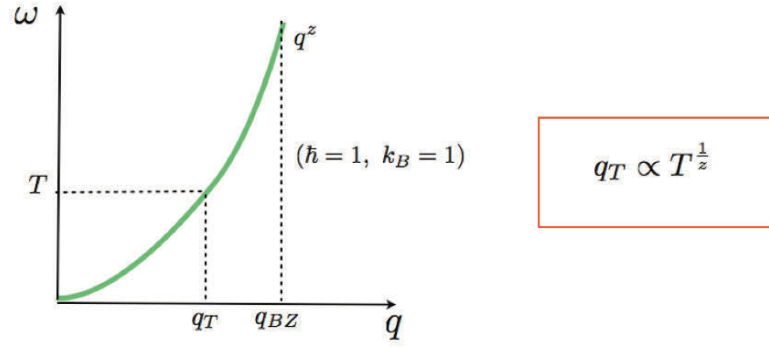
in the propagating limit where ω_q is the oscillator frequency of the mode of wavevector q , though of course more general power spectra are also possible.

We note that in (7) there are two contributions: (1) $\langle \delta\phi_T^2 \rangle$ that involves the Bose factor and is strongly temperature-dependent and (2) $\langle \delta\phi_{ZP}^2 \rangle$ due to zero-point fluctuations. Here we focus on $\langle \delta\phi_T^2 \rangle$ since it will be crucial in determining the temperature-dependence of any measured quantity. At high temperatures ($T \gg \omega$), $n_\omega \equiv T/\omega$ we obtain, by invoking causality in the form of the Kramers-Kronig relations, a generalized equipartition theorem

$$\langle \delta\phi_T^2 \rangle \approx T \sum_{q < q_{BZ}} \chi_q \quad (T \gg \omega_q \text{ for } q < q_{BZ}) \quad (9)$$

where all the modes up to the Brillouin wavevector q_{BZ} are excited; here the dynamics drop out completely of the classical equilibrium description. We note that in (9) we have a d -dimensional wavevector summation over the Brillouin zone that implies a d -dimensional theory in real space. Once quantum fluctuations are important ($T \ll \omega$), $n_\omega \approx e^{-\omega/T}$ and the dynamics remain. Now the modes will be classical up to a thermal wavevector cutoff (q_T) determined by quantum mechanics and the dispersion (see Fig. 2). More specifically the relevant wavevectors are the Brillouin zone (q_{BZ}) and the thermal (q_T) wavevectors, where the latter's temperature-dependence, determined by the condition $\omega \sim T$ and the dispersion $\omega \propto q^z$, is $q_T \propto T^{1/z}$; we note that $1/q_T$ is a generalized deBroglie wavelength that corresponds to the usual free-particle case when $z = 2$. We emphasize that the smaller of the two wavevector scales, q_T and q_{BZ} , serves as a cutoff for the classical fluctuations. If $q_T < q_{BZ}$ then not all the modes in the Brillouin zone are thermally excited; in this case the dynamical exponent enters via q_T and thus quantum fluctuations contribute to the variance of the order parameter fluctuations. Applying these ideas to (6) and again invoking Kramers-Kronig relations, we obtain

$$\langle \delta\phi_T^2 \rangle \approx T \sum_{q < q_T} \chi_q \quad (T \gg \omega_q \text{ for } q < q_{BZ}). \quad (10)$$



$q_{BZ} < q_T$ Purely Classical Fluctuations

$q_{BZ} > q_T$ Quantum Fluctuations Present

Fig. 2: Schematic of the dispersion and the important wavevectors associated with the presence of classical and quantum fluctuations.

Can we please use this approach to calculate a measurable quantity? Using a Landau-Ginzburg approach to phase transitions combined with (9) and (10), we can relate the variance $\langle \delta\phi_T^2 \rangle$ to the susceptibility χ , an observable quantity [6]; though this is currently a general discussion, we note that this treatment is appropriate for polar materials [9]. Since

$$\chi_q^{-1} \propto q_\xi^2 + q^2 \quad \Rightarrow \quad \lim_{q \rightarrow 0} \chi^{-1} \propto q_\xi^2 \quad (11)$$

where q_ξ is the inverse (classical) correlation length; we note that the latter is often denoted as κ in the literature, but we will not use this notation here since κ will be used later for other purposes. We recall that Landau theory is a symmetry-based description of macroscopic properties near a phase transition. This coarse-graining procedure ensures that the main effects of zero-point fluctuations are absorbed in the Landau coefficients, and that thermal effects appear through fluctuations of the order parameter field coarse-grained over $1/q_T$. We will assume that this scale is large enough so that a Taylor expansion of the free energy is still reasonable for our applications.

The Landau free energy density for a system with moment density ϕ and conjugate field \mathcal{E} is

$$f = \frac{1}{2}\alpha\phi^2 + \beta\frac{1}{4}\phi^4 + \frac{1}{2}\gamma|\nabla\phi|^2 - \mathcal{E}\phi \quad (12)$$

where $\alpha \rightarrow 0$ at the transition and β and γ are constants. Minimizing this free energy with respect to the order parameter ϕ , we obtain

$$\mathcal{E} = \alpha\phi + \beta\phi^3 - \gamma\nabla^2\phi. \quad (13)$$

In order to obtain $\langle \delta\phi^2 \rangle$, we follow the standard prescription of adding a random (Langevin) field to \mathcal{E} ; next we average over the random fluctuations in (13) using $\phi \rightarrow \bar{\phi} + \delta\phi$ where $\bar{\phi}$ is

the average and $\langle \phi \rangle = 0$ to obtain to lowest order

$$\mathcal{E} = (\alpha + 3\beta\langle\delta\phi^2\rangle)\bar{\phi} - \gamma\nabla^2\bar{\phi} \quad (14)$$

where we note that the variance emerges from the anharmonic cubic contribution in (13). In the limit of small $\bar{\phi}$ and \mathcal{E} , we can Fourier transform this expression to obtain

$$\chi_q^{-1} = (\alpha + 3\beta\langle\delta\phi^2\rangle) + q^2. \quad (15)$$

If we consider the $q \rightarrow 0$ limits of both (11) and (15), retaining the most temperature-dependent terms, we obtain

$$\lim_{T \rightarrow 0} q_\xi^2 \propto \langle\delta\phi_T^2\rangle \quad (16)$$

where we have assumed a quantum critical point (QCP) so that $\alpha \rightarrow 0$ as $T \rightarrow 0$. We note that (16) is only valid near a $T_c = 0$ phase transition since for a nonzero T_c there are additional terms proportional to $T_c \neq 0$ so that this expression of proportionality is no longer valid [6].

We can now combine (10), (11) and (16) to determine the temperature-dependence of the susceptibility near a quantum critical point, obtaining the expression

$$q_\xi^2 \propto \sum_{q < q_T} \frac{T}{q_\xi^2 + q^2} \approx T \int_{q_\xi}^{q_T} \frac{q^{d-1} dq}{q^2} \approx T q_T^{d-2} \left(1 - \left(\frac{q_\xi}{q_T}\right)^{d-2}\right) \quad (17)$$

where, using $q_T \propto T^{1/z}$, we would like to disregard the q_ξ/q_T term on the right-hand side of (17) so that we can write

$$\chi^{-1} \propto q_\xi^2 \propto T^{\frac{(d+z-2)}{z}} \quad \Rightarrow \quad \chi^{-1} \propto T^2 \quad (d = 3, z = 1). \quad (18)$$

where we anticipate the situation for $d = 3$ quantum paraelectrics with $z = 1$ ($\omega \propto q$). We note that this situation ($d+z = 4$) is marginal, so technically there will be logarithmic corrections though they are not observed experimentally [6, 10]. We take a moment to note that (18) is distinct from the Curie behavior ($\chi^{-1} \propto T$) observed in the approach to the classical transition.

When is this assumption valid ? We can address this question by rearranging (17) to yield

$$\left(\frac{q_\xi}{q_T}\right)^2 \propto T^{\frac{(d+z-4)}{z}} \left(1 - \left(\frac{q_\xi}{q_T}\right)^{d-2}\right) \quad (19)$$

From (19) we see that

$$\lim_{T \rightarrow 0} \left(\frac{q_\xi}{q_T}\right) = 0 \quad \text{if } d_{\text{eff}} = d+z > 4; \quad (20)$$

in this case (18) is true, and no further fluctuation effects need to be considered; there will be weak logarithmic corrections for $d+z = 4$. The upper critical dimension of this quantum theory is thus $D^u = 4-z$. In other words the inclusion of dynamics in quantum critical phenomena reduces the upper critical dimension from $d^u = 4$ in the purely classical limit; from this standpoint in experiment we are often above the upper critical dimension near a quantum phase transition in real materials.

1.2 Polar quantum criticality?

Polar materials undergo inversion symmetry-breaking transitions to phases characterized by polar space groups. Insulating ferroelectrics are among the simplest polar materials; they host spontaneous polarizations that can be switched by electric fields of practical magnitude. Furthermore ferroelectrics are in a class of polar materials whose electromechanical properties are important for transducers, passive memory components and infrared sensors. As a result of their many practical applications, they are predominantly studied at room temperature [11–15].

Can these functional materials “teach” us about some fundamental physics? Indeed historically ferroelectrics played an important role in our collective understanding of classical critical phenomena in the pioneering work of A.I. Larkin and D.E. Khmel'nitskii (LK) [16, 17]. In the sixties it was known that Landau theory breaks down for the Ising model in four or fewer dimensions, and that this model's universal behavior was equivalent to that of a ϕ^4 field theory. Exploiting this link, LK applied the renormalization methods of quantum electrodynamics to the ϕ^4 model in $d = 4$, finding clear singularities in the exponents of the specific heat and other quantities. Finally they noted that the four-dimensional Ising model is realized in a three-dimensional uniaxial ferroelectric, and indeed their results were confirmed experimentally, first in a dipolar Ising ferromagnet [18] and then later in a uniaxial ferroelectric [19].

Let us take a moment to get a flavor for the LK argument about the effective dimensionality of a uniaxial ferroelectric. Ferroelectrics are well-described by $O(n)$ (spherical) models where $d^u = 4$ is the upper critical dimension; this of course means that interactions are relevant for $d < d^u$, whereas mean-field (Landau) theory is fine for $d > d^u$ and $d^u = 4$ is marginal. Let us assume that all dipoles are in the z direction with a dipole potential $W(q) \propto q_z^2/q^2$ so that the resulting action is

$$S = \int \frac{d^3q}{(2\pi)^d} |\phi_q|^2 \left(q^2 + \frac{q_z^2}{q^2} + \Delta^2 \right) \quad (21)$$

where Δ refers to its gap. If we assume

$$q^2 \approx q_x^2 + q_y^2 = q_\perp^2 \quad (22)$$

and apply the simple scaling expressions

$$x \rightarrow bx, \quad q_\perp \rightarrow \frac{q_\perp}{b}, \quad q_z \rightarrow \frac{q_z}{b^k} \quad (b, k > 1) \quad (23)$$

then we obtain

$$S \approx \int \frac{d^2q_\perp dq_z}{b^{2+k}} |\phi_q|^2 \left(\frac{q^2}{b^2} + \frac{q_z^2}{q^2} \frac{b^2}{b^{2k}} + \Delta^2 \right). \quad (24)$$

We see that, in order for (24) to have the same form as (21), we require

$$2 - 2k = -2 \quad \rightarrow \quad k = 2 \quad (25)$$

so that q_z “counts” for effective two dimensions. In this sense the effective dimension of the uniaxial ferroelectric is $d_{\text{eff}} = d + 1$ so that a three-dimensional uniaxial ferroelectric has an effective dimension of four and is thus a setting to test predictions for the upper critical dimension

of the Ising model. More specifically, in Landau theory the specific heat has only a discontinuity ($\alpha = 0$) and LK were able to calculate the critical logarithmic corrections for the marginal case $d^u = 4$. The LK results were the first exact calculations of non-mean field exponents in an experimentally realizable systems, that subsequent measurements confirmed [18, 19].

Fine, but what can polar materials bring to the field of quantum criticality? The emergence of complex states of quantum matter in the neighborhood of zero-temperature phase transitions suggests that such quantum phenomena should be explored in a variety of settings [6]. Paraelectric (disordered) materials in close proximity to polar quantum critical points can be viewed as “economy” quantum critical systems whose propagating dynamics and few degrees of freedom allow for detailed interplay between analytic approaches, first-principles approaches and laboratory measurements. From an experimental standpoint, the pressure-sensitivity of polar transition temperatures is very appealing. For example, in order to cover a 300 K range in magnetic T_c 's, hundreds of kilobars must be applied, whereas in ferroelectrics the same temperature range can be covered with an order of magnitude less pressure. Furthermore the electric field as another “tuning knob” is significantly easier to apply than is its magnetic counterpart. Finally the dispersion $\omega \propto q$ in most ferroelectrics so that $z = 1$ which means that these materials can be studied and probed below, at and above their upper critical dimension in contrast to magnetic materials where z is typically of higher values. Additional degrees of spin and charge can be added to these polar materials, leading to rich phase behavior mostly as yet to be explored.

How old is the study of polar quantum criticality? There has been tremendous “historical entanglement” between the fields of ferroelectrics and criticality, beginning with the calculation of non-mean field exponents at marginal dimensionality that we have just discussed. Similarly the transverse-field Ising model, one of the simplest settings for a quantum critical point, was first developed to describe an order-disorder transition in the ferroelectric KH_2PO_4 [20]. Indeed there have been several “waves” of interest in low-temperature polar materials and here, for the sake of completeness and compactness, I refer interested readers elsewhere to read about these developments [6, 21].

For our purposes, let us consider a paper in 1971 by A.B. Rechester where he calculates the temperature-dependence of the dielectric susceptibility (χ) near a continuous polar phase transition [22]; to do this, he employs a parquet approximation, valid because he is working in a marginal dimension, to obtain $\chi^{-1} \propto T^2$. The key question here is whether there is a simpler way to get this result. First, we note that in our previous treatment relating $\langle \delta\phi_T^2 \rangle$ to $\chi(T)$, we obtained this same result in (18), setting $d = 3$ and $z = 1$. Strictly speaking this approach is only valid for $d+z > 4$, but since we are in the marginal dimension ($d+z = 4$) we are using it assuming, it turns out correctly, that the logarithmic corrections will not be important experimentally. We should add that long-range dipolar interactions have been neglected as their main effect near a QCP is to produce a gap in the longitudinal fluctuations; the transverse fluctuations however remain critical [16, 23].

We have already discussed the fact that temperature is *not* a tuning parameter in the vicinity of a quantum phase transition, but rather plays the role of a *finite-size boundary effect* on time. Indeed we can adapt finite-size scaling (FSS) approaches near classical phase transitions to study

Finite-Size Scaling in Space and in Time

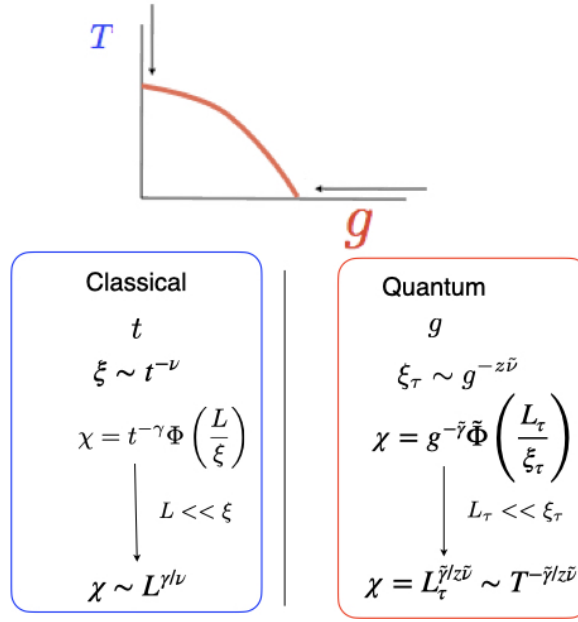


Fig. 3: Schematic of finite-size scaling at classical and at quantum critical points.

the influence of temperature near a QCP. This scaling approach is strictly valid in dimensions for $d+z < 4$, so again we will argue that because $d = 3$ quantum critical paraelectrics are marginal ($d+z = 4$), the scaling results are valid up to logarithmic corrections. Following the standard FSS procedure [24], we impose boundaries on the system near its critical point. For a classical system with tuning parameter $t = T/(T-T_c)$ and correlation length $\xi \sim t^{-\nu}$, we confine it in a box of size L and then write the standard FSS scaling form

$$\chi \sim t^{-\gamma} \Phi\left(\frac{L}{\xi}\right) \sim t^{-\gamma} \Phi\left(\frac{L}{t^{-\nu}}\right). \quad (26)$$

For $L \ll \xi$, we must have $\chi = \chi(L)$ and assuming that $\Phi(x) \sim x^p$, we obtain

$$\chi \sim t^{-\gamma} \left(\frac{L}{\xi}\right)^p \sim t^{-\gamma} \left(\frac{L}{t^{-\nu}}\right)^p \sim L^{\frac{\gamma}{\nu}}. \quad (27)$$

Now let us apply the analogous finite-size scaling to time near a quantum critical point. We note that

$$\xi \sim g^{-\tilde{\nu}} \quad \rightarrow \quad \xi_\tau \sim g^{-z\tilde{\nu}} \quad (\omega \propto q^z \rightarrow [\xi_\tau] = [\xi^z]) \quad (28)$$

where g is the tuning parameter of the quantum phase transition, ξ_τ is the correlation time, and we write the exponents for the quantum transition with a tilde (e.g. $\tilde{\nu}$) to distinguish them from their classical counterparts (ν); we now have the boundary cutoff in time $L_\tau = \tau_P = \hbar/(k_B T)$ that is inversely proportional to temperature. Then the scaling expression for the susceptibility is

$$\chi \sim g^{-\tilde{\gamma}} \Phi\left(\frac{L_\tau}{\xi_\tau}\right) \sim g^{-\tilde{\gamma}} \Phi\left(\frac{L_\tau}{g^{-z\tilde{\nu}}}\right). \quad (29)$$

Then for $L_\tau \ll \xi_\tau$ we must have $\chi = \chi(L_\tau)$ so that we obtain

$$\chi \sim g^{-\tilde{\gamma}} \left(\frac{L_\tau}{\xi_\tau} \right)^p \sim g^{-\tilde{\gamma}} \left(\frac{L_\tau}{g^{-z\nu}} \right)^{\frac{\tilde{\gamma}}{z\tilde{\nu}}} \sim L_\tau^{\frac{\tilde{\gamma}}{z\tilde{\nu}}} \sim T^{-\frac{\tilde{\gamma}}{z\tilde{\nu}}} \quad (30)$$

at finite temperature near a polar QCP; here $z = 1$, $\tilde{\nu} = \frac{1}{2}$ and $\tilde{\gamma} = 1$ so that $\tilde{\gamma}/(z\tilde{\nu}) = 2$ and $\chi^{-1} \propto T^2$.

In summary, exploiting the fact that the $d = 3$ quantum critical paraelectrics reside in its marginal dimension, we have used both mean-field and scaling arguments to recover the $1/T^2$ behavior of the dielectric susceptibility near a polar quantum critical point that was previously derived using more technical diagrammatic, large N and renormalization group methods [6]; it has also been observed experimentally, validating our neglect of logarithmic corrections [6, 10].

The Rundown. So why should we explore polar quantum criticality? Of course in our collective quest for universality, it is important to study quantum phase transitions in many different settings. Furthermore polar quantum critical materials offer the following opportunities:

- Simple “economy” examples with few degrees of freedom and non-dissipative dynamics.
- Their linear dispersion ($z = 1$) means that they can be studied at, below and above their upper critical dimension allowing for a detailed interplay between theory and experiment.
- Additional degrees of freedom like spin and charge can be added systematically.

However there are also outstanding conceptual questions that include

- How can systems that display classical first-order phase transitions display quantum criticality?
- Can metals near polar quantum criticality host novel strongly correlated phases?

These issues motivate our discussion in the subsequent sections of this chapter.

2 Quantum annealed criticality

2.1 The challenge: classical first-order transitions!

Let us start simply with polar insulators. At finite temperatures and ambient pressure these materials typically display first-order transitions due to strong electromechanical coupling [11–13]; yet in many cases their dielectric susceptibilities indicate the presence of pressure-induced quantum criticality associated with zero-temperature quantum phase transitions [6, 10]. The interplay of first-order phase transitions with quantum fluctuations is known to lead to exotic quantum states near quantum critical points. In many metallic quantum ferromagnets, coupling of the local magnetization to the low-energy particle-hole excitations transforms a high-temperature continuous transition into a low-temperature discontinuous one, and the resulting classical tricritical points have been observed in many systems [25].

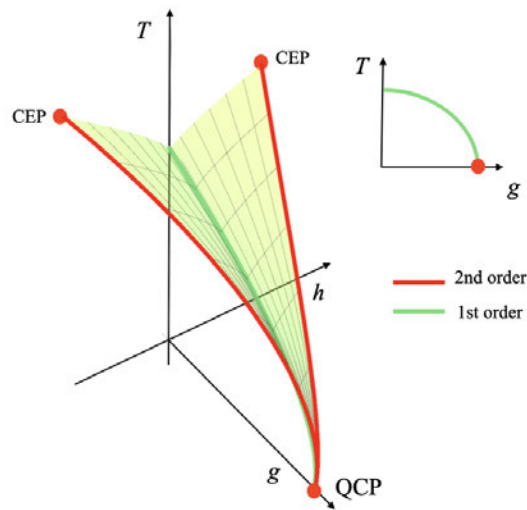


Fig. 4: *Temperature (T)-Field (h)-Tuning Parameter (g) Phase Diagram with a sheet of first-order transitions bounded by critical end-points (CEP) terminating at a zero temperature quantum critical point (QCP); here g tunes the quantum fluctuations and h is the field conjugate to the order parameter. Inset: Temperature-Tuning Parameter “slice” indicating a line of classical phase transitions ending in a “quantum annealed critical point” where the underlying order parameter criticality is restored by zero-point fluctuations.*

In this section, we will discuss a theoretical basis for the observation that many polar insulators display quantum critical behavior despite hosting classical first-order transitions. Experimentally it is known that classical ferroelectric transitions, for example in BaTiO_3 , are continuous when clamped and become first-order when unclamped [12]. In magnetic systems there is a mechanism, studied by A.I. Larkin and S.A. Pikin (LP), where strain-energy density coupling is known to drive discontinuous transitions in compressible systems that are critical when clamped [26]. We will adapt this Larkin-Pikin approach to (compressible) polar systems and ask what happens in the approach to zero temperature. In a nutshell, we will show that as the temperature is lowered, quantum fluctuations reduce the amplitudes of their thermal counterparts, weakening the first-order transition and “annealing” the system’s elastic response, ultimately resulting in a $T = 0$ “quantum annealed” critical point. As we will see, this is because fluctuations at finite temperature are more singular than at $T = 0$ where the effective dimension is higher than in the classical case. The general temperature (T)-tuning parameter (g)-field (h) phase diagram that emerges is presented in Fig. 4 where the field (h) is conjugate to the order parameter. A flavor of this theoretical underpinning to the observed behavior will be given here where details are available elsewhere for the interested reader [27].

2.2 Adaptation of the Larkin-Pikin approach

Before we adapt it, what is the classical Larkin-Pikin approach? At a first-order transition the quartic mode-mode coupling of the effective action becomes negative. One mechanism for this phenomenon, studied by Larkin and Pikin [26] (LP), involves the interaction of strain with the fluctuating energy density of a critical order parameter. LP found that a diverging specific heat in the “clamped” (fixed volume) system leads to a first-order transition in the unclamped

system at constant pressure. The Larkin-Pikin criterion [26] for a first order phase transition is

$$\kappa \lesssim \frac{\Delta C_V}{T_c} \left(\frac{dT_c}{d \ln V} \right)^2 \quad (31)$$

where V is the volume, ΔC_V is the singular part of the specific heat capacity in the clamped critical system, T_c is the transition temperature and $dT_c/d \ln V$ is its volume strain derivative. The effective bulk modulus κ is defined by $\kappa^{-1} = K^{-1} - (K+4\mu/3)^{-1}$ where K and μ are the bare bulk and the shear moduli in the absence of coupling between the order parameter and strain; physically $\kappa \sim K c_L^2 / c_T^2$ where c_L and c_T are the longitudinal and the transverse sound velocities. More specifically, LP considered the coupling

$$\mathcal{L}_I = \lambda e_{ll}(\vec{x}) \psi^2(\vec{x}) \quad (32)$$

between the volumetric strain field e_{ll} and the squared amplitude ψ^2 of the critical order parameter. In a critical system, the singular fluctuations of the energy density are directly proportional to ψ^2 ; thus (32) corresponds to a strain-energy coupling. Naively (32) is expected to induce a short-range attractive order parameter interaction. LP showed that (32) also leads to an anomalous long-range interaction between order parameter fluctuations; careful integration, as we shall discuss, over the elastic degrees of freedom results in a qualitative transformation of the action

$$S \longrightarrow S - \frac{\lambda^2}{2T\kappa} \left[\frac{1}{V} \int d^3x \int d^3x' \psi^2(\vec{x}) \psi^2(\vec{x}') \right] \quad \text{with} \quad \frac{1}{\kappa} = \left(\frac{1}{K} - \frac{1}{K+4\mu/3} \right) \quad (33)$$

where μ is the shear modulus [26, 27]. This long-range interaction is finite if $\mu > 0$, i.e., if the medium is a solid. LP showed that this induced long-range interaction in (33) generates positive feedback to the tuning parameter, leading to a multi-valued free energy surface and a resulting first order phase transition.

To summarize the situation more conceptually, we note that in the LP scenario the strain-energy density coupling results in a renormalized effective bulk modulus

$$\tilde{\kappa} \equiv \kappa - \Delta\kappa \quad (34)$$

in the unclamped system where the shift in the effective bulk modulus is related to the singular part of the (clamped) specific heat

$$\Delta\kappa = \frac{\Delta C_V}{T_c} \left(\frac{dT_c}{d \ln V} \right)^2. \quad (35)$$

The condition for a macroscopic instability, and hence a first-order transition, is when the renormalized bulk modulus is negative

$$\kappa - \Delta\kappa = 0 \quad \Rightarrow \quad \kappa \lesssim \frac{\Delta C_V}{T_c} \left(\frac{dT_c}{d \ln V} \right)^2 \quad (36)$$

and we see that we have recovered the LP criterion (31). Here we note that it is the divergence of $\Delta\kappa$ that is crucial to this result.

The LP criterion in its current form is not appropriate for T=0! When we generalize the Larkin-Pikin approach to include quantum zero-point fluctuations of the energy density, we show that it is the divergence of the energy fluctuations, both quantum and classical, that is crucial for the LP mechanism [27]. When we sum over all possible spacetime configurations in the action, we obtain a generalized LP criterion

$$\kappa \lesssim \left(\frac{dg_c}{d \ln V} \right)^2 \chi_{\psi^2} \quad (37)$$

where

$$\chi_{\psi^2} = \int_0^\beta d\tau \int d^3x \langle \delta\psi^2(\vec{x}, \tau) \delta\psi^2(0) \rangle \quad (38)$$

is the space-time average of the quantum and thermal “energy” fluctuations, $\beta = \frac{1}{k_B T}$ and g is the tuning parameter for the quantum phase transition, with the convention that $g_c(T=0) = 0$. At zero temperature, this expression extends the original LP criterion (36) to quantum phase transitions. As we will discuss further shortly, at finite temperatures, the critical quantum and classical tuning parameters are related by $g_c(T_c) = u T_c^{1/\tilde{\Psi}}$, where $\tilde{\nu}$ and z are the exponents associated with the quantum correlation length and the dynamics respectively and $\tilde{\Psi} = \tilde{\nu}$ is called the shift exponent [4]; therefore $d \ln g_c = \frac{1}{\tilde{\Psi}} d \ln T_c$ and the LP criterion becomes

$$\kappa - \Delta\kappa = 0 \quad \Rightarrow \quad \kappa \lesssim \left(\frac{dT_c}{d \ln V} \right)^2 \overbrace{\left(\frac{g}{2T_c} \right)^2}^{\Delta C_v/T_c} \chi_{\psi^2}, \quad (39)$$

where we have identified $\Delta C_v/T_c = (g/2T_c)^2 \chi_{\psi^2}$ with the specific heat capacity. In this way, we see that the generalized Larkin-Pikin equation encompasses the original criterion (31) in addition to being applicable at low temperatures [27]. Due to their additional time dimension, quantum fluctuations are typically less singular than are their classical counterparts. As the temperature is lowered, the correlation volume of the zero-point fluctuations grows, reducing the amplitudes of the singular thermal fluctuations in the clamped system. The induced first order transition thus becomes progressively weaker with decreasing temperature, leading to a continuous “quantum annealed” transition at $T = 0$.

Is there a simple way to get a sense of the quantum Larkin-Pikin result? We have seen that the LP criterion can be reexpressed as

$$\kappa - \Delta\kappa = 0 \quad (40)$$

We can use a scaling argument to get a flavor for the key quantum LP result. Let us rewrite (39) as

$$\tilde{\kappa} = \kappa - \Delta\kappa = \kappa - \gamma^2 \chi_{\psi^2} \quad (41)$$

with

$$\chi_{\psi^2} = \int_0^\beta d\tau \int d^d x \langle \delta\psi^2(\vec{x}, \tau) \delta\psi^2(0) \rangle, \quad (42)$$

where we have generalized the expression (38) to d spatial dimensions. If we make the Gaussian approximation $\langle \delta\psi^2(\vec{x}) \delta\psi^2(0) \rangle \approx (\langle \delta\psi(\vec{x}) \delta\psi(0) \rangle)^2$, then the zero-temperature limit of χ_{ψ^2} is

$$\lim_{T \rightarrow 0} \chi_{\psi^2} \approx \int d\tau d^d x (\langle \delta\psi(\vec{x}) \delta\psi(0) \rangle)^2 = \int \frac{d\nu}{2\pi} \frac{d^d q}{(2\pi)^d} (\chi_{\psi}(\vec{q}, \nu))^2 \quad (43)$$

where we have Fourier transformed into momentum space, and $\chi_{\psi}(\vec{q}, \nu) = \langle \delta\psi(-q) \delta\psi(q) \rangle$, the order parameter susceptibility, is the space-time Fourier transform of the correlator $\langle \psi(\vec{x}) \psi(0) \rangle$. It then follows that

$$\lim_{T \rightarrow 0} \Delta\kappa \propto \int dq d\nu q^{d-1} (\chi_{\psi}(\vec{q}, i\nu))^2. \quad (44)$$

To examine how this quantity behaves in the approach to the quantum critical point of the clamped system, we can use dimensional power-counting. Since $[\chi] = [\frac{1}{q^2}]$ and $[\nu] = [q^z]$,

$$\lim_{T \rightarrow 0} [\Delta\kappa] = \frac{[q^{d+z}]}{[q^4]} \sim \xi_Q^{4-(d+z)}$$

where we have replaced $[q^{-1}] = [\xi_Q]$, the quantum correlation length. As the quantum critical point of the clamped system is approached, $\xi_Q \rightarrow \infty$, so that the quantum corrections to κ are non-singular for $d+z > 4$; in this case $\Delta\kappa$ does not diverge so a continuous transition is possible. Of course for three-dimensional polar insulators with a linear dispersion $d+z = 4$ is marginal, so there will be logarithmic corrections; this suggests that the quantum phase transition will be very weakly first-order which may be indistinguishable from continuous in experiment. Basically here we are arguing that if the $T = 0$ compressible system lies above its upper critical dimension, the line of first-order transitions can end in a “quantum annealed critical point” where zero-point fluctuations restore the underlying criticality of the order parameter.

How can this scaling argument be substantiated? This scaling logic can be supported by a more technical argument which we will now outline; here we consider the simplest case: isotropic elasticity and a scalar order parameter ψ . The action, $\mathcal{S}[\psi, u]$ is then a function of ψ and u , the lattice displacement; it has three distinct components corresponding to the physics of ψ , a description of the elastic degrees of freedom and finally the strain-energy density coupling with strength λ [26, 27]. The generalized LP argument is subtle and proceeds in three steps:

- Careful integration of the $q = 0$ and $q \neq 0$ Gaussian strain contributions distinctly.
- Identification of an expression relating the unclamped and the clamped free energies.
- Use of crossover scaling [4] to determine $T \rightarrow 0$ phase behavior when both classical and quantum critical fluctuations are present.

Here the key first step is to integrate out the Gaussian elastic degrees of freedom from the action

$$Z = \int \mathcal{D}[\psi] \int \mathcal{D}[u] e^{-\mathcal{S}[\psi, u]} \rightarrow Z = \int \mathcal{D}[\psi] e^{-S[\psi]} \quad (45)$$

where the actions involve integrals over spacetime. This procedure must be performed with some care because of the special role of boundary normal modes. In a solid of volume L^3 , the

normal modes can be separated into two components according to their wavelength λ : sound waves with $\lambda \ll L$ and boundary waves with $\lambda \sim L$. From another perspective, we can understand this distinction by noting that the strain only couples to the longitudinal modes; however at $q = 0$ there is no distinction between transverse and longitudinal modes so this case must be treated separately from the finite- q situation.

The generalized Larkin-Pikin action, following careful integration of the Gaussian strain to include both thermal and quantum fluctuations, is

$$S[\psi] = S_L[\psi, \tilde{g}, b^*] - \frac{\lambda^2}{2} \left(\frac{1}{K} - \frac{1}{K + 4\mu/3} \right) \frac{1}{\beta V} \int d^4x \int d^4x' \psi^2(\vec{x}) \psi^2(\vec{x}'). \quad (46)$$

with the local contribution

$$S_L[\psi, \tilde{g}, b^*] = \int d^4x \mathcal{L}_L[\psi, \tilde{g}, b^*] = \int d^4x \left(\frac{1}{2} (\partial_\mu \psi)^2 + \frac{\tilde{g}}{2} \psi^2 + \frac{b^*}{4!} \psi^4 \right) \quad (47)$$

where

$$b^* = b - \frac{12\lambda^2}{K + 4\mu/3}. \quad (48)$$

(46) is a $d+z$ -dimensional generalizations of the classical LP action where all spacetime configurations are summed. The essence of the Larkin-Pikin effect is the appearance of a distance-independent interaction between the energy densities of the order parameter field that appears in (46). Since the Larkin-Pikin argument is valid for arbitrarily small coupling λ , the perturbative $O(\lambda^2)$ renormalization of the short-range interaction in (48) becomes negligibly small in this limit and can be safely neglected.

The Larkin-Pikin term in (46) is a kind of “elastic anomaly”, whereby the integration over boundary modes generates nonlocal interactions between energy densities of the order parameter similar in form to (42). Indeed this distance-independent term in (46) can be written as the spacetime volume average of the energy density

$$\Psi^2 \equiv \frac{1}{\beta V} \int d^4x \psi^2(x) \quad (49)$$

that is an intensive variable with small fluctuations about its thermal average $\langle \Psi^2 \rangle$. We perform a Hubbard-Stratonovich transformation of the spacetime-independent interaction in (46)

$$- \frac{\lambda^2}{2} \frac{1}{\kappa} \frac{1}{\beta V} \int d^4x \int d^4x' \psi^2(\vec{x}) \psi^2(\vec{x}') \rightarrow \int d^4x \left((\lambda\phi) \psi^2(\vec{x}) + \frac{\kappa}{2} \phi^2 \right) \quad (50)$$

where we have introduced an auxiliary “strain” field

$$\phi = - \frac{\lambda \langle \Psi^2 \rangle}{\kappa} \quad (51)$$

that is independent of space and time. Then we may write

$$\mathcal{Z} = e^{-\beta \bar{\mathcal{F}}} = e^{-\bar{S}(\phi)} = \int \mathcal{D}\psi e^{-S[\psi, \phi]}, \quad (52)$$

where $\tilde{\mathcal{F}}$ is the free energy of the unclamped system; here

$$S[\psi, \phi] = \int d^4x \left(\mathcal{L}_L(\psi, \tilde{g}) + \lambda\phi\psi^2 + \frac{\kappa}{2}\phi^2 \right) \quad (53)$$

that can be reexpressed as

$$S[\psi, \phi] = \int d^4x \mathcal{L}_L(\psi, \tilde{g} + 2\lambda\phi) + \frac{\kappa V\beta}{2}\phi^2. \quad (54)$$

In their original classical treatment, Larkin and Pikin observed that the main effect of elasticity in the unclamped system is to make a parametrized shift of the original tuning parameter to a parametrized variable X ; we can see this in our generalized LP equations. From (52) and (54), we can write the free energy for our unclamped system as

$$\tilde{\mathcal{F}}[\phi, \tilde{g}] = \mathcal{F}[X] + \frac{\kappa V}{2}\phi^2 \quad (55)$$

where \mathcal{F} is the free energy of the clamped system and

$$X = \tilde{g} + 2\lambda\phi \quad (56)$$

indicates the shift of the tuning parameter \tilde{g} due to the presence of energy fluctuations. Now

$$\frac{1}{V} \frac{\partial \mathcal{F}}{\partial X} = \frac{\langle \Psi^2 \rangle}{2} \quad (57)$$

so that

$$\phi = -\frac{\lambda \langle \Psi^2 \rangle}{\kappa} = -\frac{2\lambda}{V\kappa} \left(\frac{\partial \mathcal{F}}{\partial X} \right) \equiv -\frac{2\lambda}{V\kappa} \mathcal{F}'[X] \quad (58)$$

where we have defined $\mathcal{F}'[X] \equiv \left(\frac{\partial \mathcal{F}}{\partial X} \right)$ for simplicity. Therefore

$$\tilde{\mathcal{F}} = \mathcal{F}[X] + \frac{2\lambda^2}{V\kappa} (\mathcal{F}'[X])^2 \quad (59)$$

and

$$X = \tilde{g} - \frac{4\lambda^2}{V\kappa} \mathcal{F}'[X]. \quad (60)$$

Let us define

$$\tilde{f} \equiv \frac{2\lambda}{V\kappa} \tilde{\mathcal{F}} \quad \text{and} \quad f \equiv \frac{2\lambda}{V\kappa} \mathcal{F}. \quad (61)$$

Here we recall that the integrals in the action involve an integral over time, $\int d^4x = \int_0^\beta d\tau \int d^3x$ where $\beta = 1/T$ is a boundary term, so that these free energies are determined at fixed temperature. Therefore the two equations describing the unclamped system are

$$\tilde{f} = f[X, T] + \lambda (f'[X, T])^2 \quad (62)$$

and

$$\tilde{g} = X + 2\lambda f'[X, T] \quad (63)$$

which have to be solved self-consistently.

Although the phase transition of the unclamped system is continuous in X , the physical tuning parameter, $\tilde{g}[X]$, can become a non-monotonic function of X , leading to a first-order transition. Thus the Larkin-Pikin criterion is

$$\frac{d\tilde{g}}{dX} = 1 - \frac{\lambda^2 V}{\kappa} \chi_{\psi^2} \quad (64)$$

where

$$\chi_{\psi^2} = \int_0^\beta d\tau \int d^3x \langle \delta\psi^2(\vec{x}) \delta\psi^2(0) \rangle \quad (65)$$

is the space-time average of the quantum and thermal “energy” fluctuations that is familiar from our previous discussion. The condition $\frac{d\tilde{g}}{dX} \leq 0$ corresponds to the development of a first-order transition; we already know that for $d+z > 4$ the term χ_{ψ^2} does not diverge so there is the possibility of a continuous transition. We note that in the physically important case of $d+z = 4$ there will be weak logarithmic effects that are probably not observable experimentally. Again here a flavor for the technical argument has been presented as a sketch, and more details are available for the curious reader [27].

2.3 Quantum annealing of the first-order transition

A crucial feature of the LP approach is that the feedback of the energy fluctuations can be understood purely by studying the critical behavior of the clamped system. In order to illustrate this, let us return to the original LP classical version of the two equations, (62) and (63)

$$\tilde{f} = f[x] + \lambda(f'[x])^2 \quad (66)$$

and

$$t = x + 2\lambda f'[x] \quad t \equiv \frac{T - T_c}{T_c} \quad (67)$$

describing the unclamped system that must be solved self-consistently. In the classical clamped system, we assume a continuous transition so we can write

$$f \propto -|t|^{2-\alpha} \quad (\alpha > 0). \quad (68)$$

Combining (67) and (68), we obtain

$$t = x + 2\lambda f'[x] = x - 2\lambda(2-\alpha) |x|^{1-\alpha} \text{sign}(x) \quad (69)$$

that is non-monotonic leading to a first-order transition for the unclamped system (see Fig. 5). Therefore, in order to generalize the Larkin-Pikin argument to $T \rightarrow 0$, we need to introduce a crossover scaling form for the clamped free energy f in (62) and (63) that is applicable near both the classical and the quantum critical points. The approach we outline here that describes both the quantum and classical cases was adapted from an earlier study used to describe Ising anisotropy at a Heisenberg critical point [4]. From our previous discussion, we recall that at a finite temperature T , the criticality of quantum fluctuations is cut off by the Planck time $\tau_P = \hbar/(k_B T)$ with a corresponding quantum correlation length $\xi_Q \sim \tau_P^{1/z}$. Near the quantum

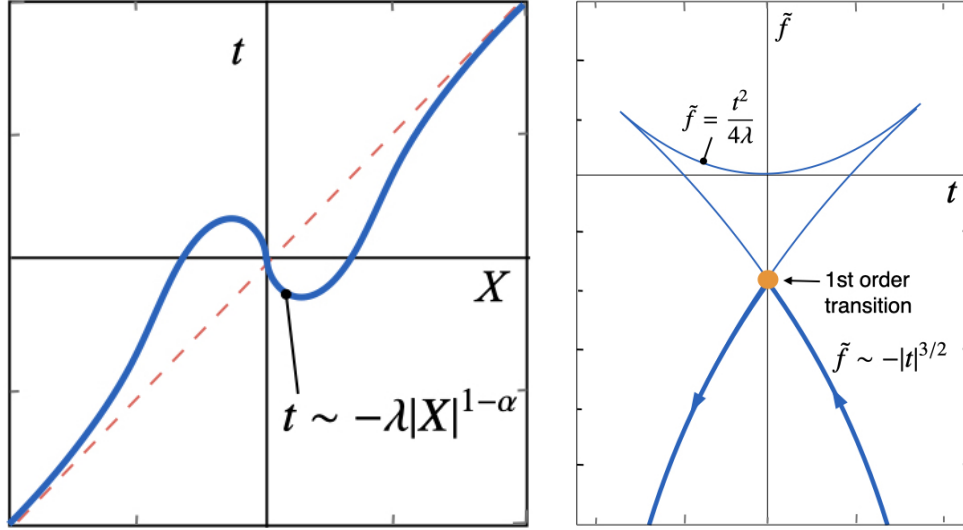


Fig. 5: Schematic of the (left) nonmonotonic relationship between the reduced temperature (t) and the parametrized variable (X) shifted by energy fluctuations for the unclamped LP problem and (right) the free energy of the unclamped compressible system for $\alpha = 1/2$ as in the original LP paper [26].

critical point at $T = 0$, the zero-point fluctuations are governed by a finite correlation length $\xi_Q \sim (g - g_c(0))^{-\tilde{\nu}}$, where g is the parameter that tunes the quantum transition and $g = g_c(0)$ is the location of the quantum critical point. If we combine our expressions for the quantum correlation length in the ordered phase close to the line of phase transitions, we find

$$(g - g_c)^{-\tilde{\nu}} \sim \left(\frac{\hbar}{k_B T_c} \right)^{1/z} \quad (70)$$

which leads to

$$T_c \sim (g - g_c)^{\tilde{\nu}z} \equiv (g - g_c)^{\tilde{\Psi}} \quad (71)$$

where $\tilde{\Psi}$ is called the shift exponent that we have discussed earlier. Therefore at finite temperature, the location of the phase transition is shifted by the thermal fluctuations, so that

$$g_c(T) = g_c(0) - uT^{1/\tilde{\Psi}}. \quad (72)$$

For convenience, we will shift the definition of g to absorb the zero temperature QCP critical coupling constant, $g_c(0)$, i.e. $g - g_c(0) \rightarrow g$, so that $g_c(T) = -uT^{1/\tilde{\Psi}}$. Now temperature is a finite size correction to the quantum critical point, and the free energy is determined by a crossover function

$$f(g, T) = g^{2-\tilde{\alpha}} \Phi \left(\frac{T^{1/\tilde{\Psi}}}{g} \right). \quad (73)$$

which describes both the quantum critical point, and the finite temperature classical critical point of the clamped system (see Figure 6); here we will use the convention that an exponent with a tilde refers to the quantum case so that α and $\tilde{\alpha}$ are classical and quantum exponents, respectively. A key point is that at finite temperature, critical behavior now occurs at the shifted

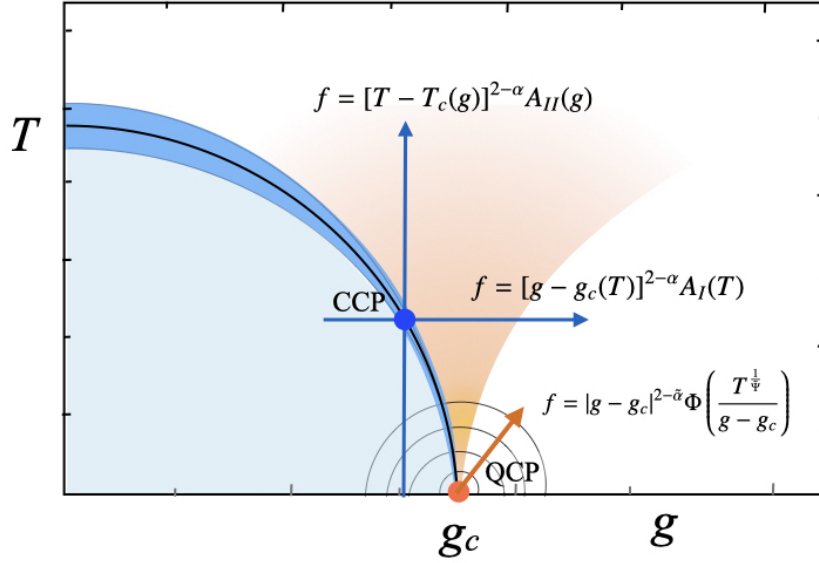


Fig. 6: Schematic showing the dependence of the free energy of the clamped system in the vicinity of the quantum critical point. The scaling function about the QCP determines the amplitude factors for the finite temperature classical critical point (CCP), given by $A_I(T)$ for a constant temperature sweep and $A_H(g)$ for a sweep at constant tuning parameter. Here the location of the quantum critical point at $g_c(0)$ is labelled as simply g_c .

value of $g_c(T)$, and the scaling behavior is governed by the finite temperature critical exponents. Therefore for a fixed temperature scan (Fig. 6) for small $g - g_c(T)$,

$$f(g, T) = (g - g_c(T))^{2-\alpha} A_I(T). \quad (74)$$

where $A_I(T)$ is the amplitude factor for the classical critical point occurring at $g = g_c(T)$. Similarly if we perform a sweep through the phase transition at constant coupling constant g (Fig. 6), then we can write

$$f[g, T] \sim (T - T_c[g])^{2-\alpha} A_H(g), \quad (75)$$

where $A_H(g)$ is amplitude factor for the quantum transition at $T_c[g] = (-g/u)^{\tilde{\Psi}}$. The scaling form (73) allows us to determine the form of these amplitude factors.

Using this crossover approach, we can study how the discontinuities in the entropy and the volume, $\Delta S(T_c)$ and $\Delta V(T_c)$, evolve along the first order phase boundary as the transition T_c is lowered towards zero. In this discussion, we shall identify the tuning parameter g with the pressure P , $g \equiv P - P_c$. Using Maxwell's relations we have

$$\frac{dT_c}{dP_c} \equiv \frac{dT_c}{dg_c} = - \left. \frac{\Delta V}{\Delta S} \right|_{T=T_c} \longrightarrow \frac{dT_c}{dg_c} \propto -T_c^{1-1/\tilde{\Psi}}. \quad (76)$$

where we have used (72) to obtain the right-hand expression in (76). For the case of polar insulators, $\tilde{\Psi} = \tilde{\nu}z = 1/2$, and we see that this $dT_c/dP_c \propto T_c^{-1}$; naively this implied divergence of $\Delta V/\Delta S$ as $T_c \rightarrow 0$ might be taken as evidence that the tendency towards a first order transition increases as the temperature goes to zero. However the paradox is resolved by noting that ΔS and ΔV simply vanish at different rates, still signifying an approach to a continuous

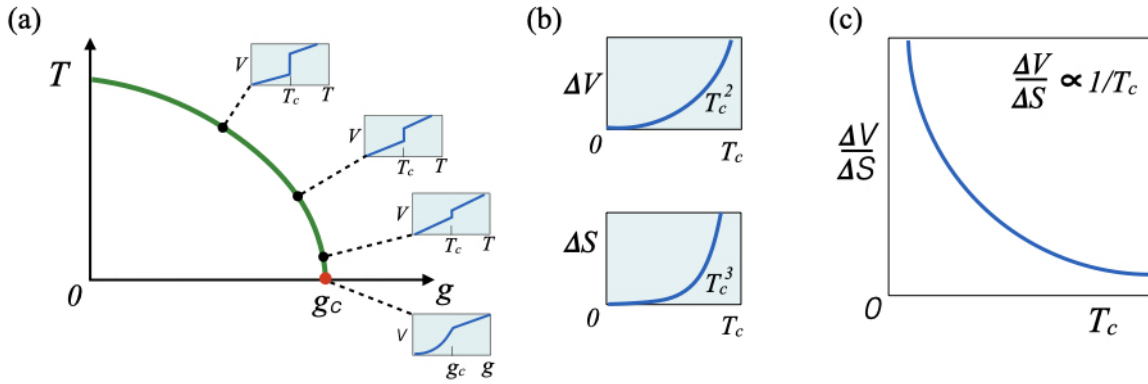


Fig. 7: Schematic figure showing the evolution of the first order phase transition in the approach to the quantum annealed critical point for the case $\tilde{\Psi} = \tilde{\nu}z = 1/2$, $\alpha = 1/2$, $\tilde{\alpha} = 0$. (a) Evolution of jump in volume (b) dependence of ΔV and ΔS on T_c and (c) T_c dependence of $\Delta V/\Delta S$.

quantum phase transition. In particular using this crossover scaling we can show [27]

$$\Delta V(T_c) \propto -T_c^{\frac{\alpha - \tilde{\alpha}}{\alpha \tilde{\Psi}}}, \quad (77)$$

so that as long as $\alpha > \tilde{\alpha}$,

$$\lim_{T_c \rightarrow 0} \Delta V \rightarrow 0 \quad (78)$$

and there is no latent work as T_c goes to zero, indicating that quantum fluctuations “anneal” the zero-temperature quantum phase transition to become continuous (Fig. 7).

The Rundown. In summary, we have developed a theoretical framework to describe compressible insulating systems that have classical first-order transitions and display pressure-induced quantum criticality. We have generalized the Larkin-Pikin approach [26] to the quantum case using crossover scaling forms that can describe both its classical and its quantum critical behavior. In particular when the system is above its upper critical dimension, there is no latent work at the quantum transition indicating that it is continuous. The key point is that a compressible material can host a quantum critical phase even if it displays a first-order transition at ambient pressure. More generally the order of a lattice-sensitive system’s classical phase transition can be different from its quantum counterpart. As always there are always outstanding questions that emerge; they include:

- Lines of discontinuous classical transitions ending in quantum critical points have now also been observed in several metallic systems; can this quantum annealed criticality approach be generalized to include electronic degrees of freedom?
- Can this LP mechanism be understood in a broader field-theoretic context? It has a topological flavor since a $q = 0$ “boundary component of the strain drives the long-range interaction; when integrated around a closed loop on a torus, it is a topological invariant that counts the number of enclosed defect [27]. This appears to be a sort of bulk-boundary correspondence thus suggesting a phenomenon that is topological in character and should be explored.

3 Novel metallicity

So far, we have only discussed polar insulators. However now let us turn to the other conceptual question we posed earlier: Can metals near polar quantum criticality host novel strongly correlated phases?

What exactly is a polar metal and do they exist? A polar metal undergoes a continuous transition from a non-polar to a polar crystal structure; there is no macroscopic polarization due to screening by the conduction electrons [30–32]. Though predicted some time ago [30], it is only relatively recently that such polar metals have been identified experimentally and there exist both intrinsic and engineered varieties with many more predicted [31, 32]. In the extrinsic case, charge can be added to a polar insulator by either chemical and/or gate doping. The Mott criterion for the critical dopant concentration (n_c) for a metal-insulator transition in doped (3d) semiconductors occurs when the average dopant-dopant distance ($d = n^{-1/3}$) is a significant fraction of the effective Bohr radius ($a_B^* = \epsilon \hbar^2 / (m^* e^2)$) where ϵ is the dielectric constant; more concretely the critical concentration n_c is defined as $a_B^* n_c^{1/3} \approx 0.26$, consistent with experiment in many semiconductors [28]. Since the effective Bohr radius is proportional to the dielectric constant (ϵ), it is much larger in materials near polar transitions like n-doped STO than in doped semiconductors based on silicon or germanium (see Figure 8); therefore a lower n_c is expected, consistent with observation [29, 28]. Polar metals can thus have very low carrier concentrations.

Is polar quantum criticality experimentally accessible? Polar transition temperatures of metallic systems have been controllably suppressed, driving them into observed quantum critical regimes [33, 34]. Metals close to quantum critical points are known to be strongly correlated systems that host exotic phases including non-Fermi liquids and unconventional superconductivity where specifics depend on the nature of the quantum criticality involved [25, 35]. The vicinities of polar quantum critical points thus present new settings to explore such novel metallicities [36].

3.1 The challenge: how to couple electrons to a soft polar mode?

In quantum critical polar metals, the $q = 0$ soft mode is an inversion symmetry-breaking transverse optical phonon that has no direct coupling to the charge density. Furthermore the usual Fröhlich electron-phonon coupling vanishes for $q \rightarrow 0$. Quantum critical polar metals thus offer opportunities to study novel electron-phonon interactions and their resulting collective behaviors. A key challenge in studying novel metallicity near polar quantum critical points is how to promote strong electronic coupling to the critical polar mode. Conversely, the region around a polar quantum critical point presents an opportunity to explore nontraditional electron-phonon interactions; proposed couplings that include order parameter gradients and/or nonlinearities are usually irrelevant in the scaling sense at a QCP, leading to Fermi liquid behavior. Additionally, Coulomb interactions play a special role here, gapping the longitudinal mode when the screening is weak [16, 23].

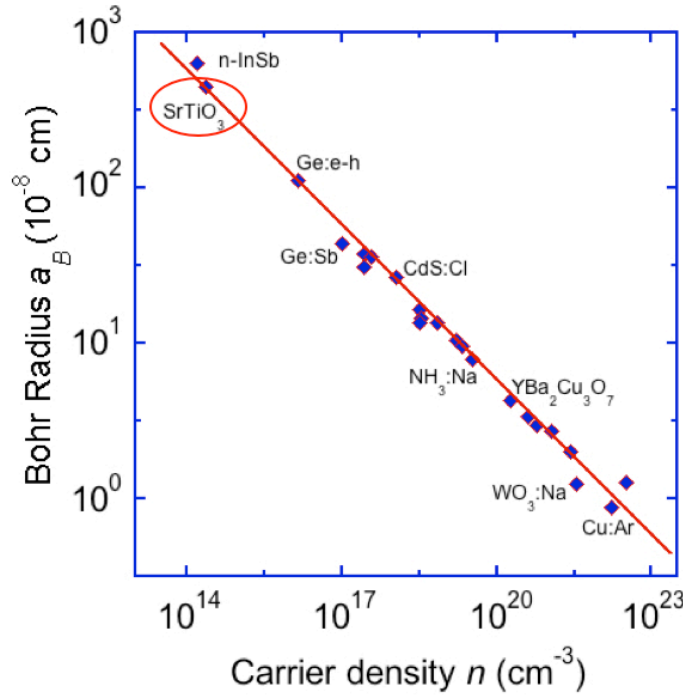


Fig. 8: A plot of the effective Bohr radius (a_B) vs. carrier density (n) indicating good comparison between the Mott criterion ($n_c^{1/3} a_B = 0.26$) for the metal-insulator transition in a number of experimental systems. Here $a_B = \epsilon \hbar^2 / (m^* e^2)$ is determined experimentally whenever possible using spectra, otherwise computationally, and the critical carrier density (n_c) for metallicity is measured [28]. Because the effective Bohr radius is proportional to the dielectric constant, it is large for a doped nearly polar material like n - SrTiO_3 ; this results in a low critical carrier concentration for the metal-insulator transition consistent with observation [29]. (Adapted from [28] with permission from the American Physical Society.)

3.2 Spin-orbit assisted electron-phonon interactions

Many anomalous properties of quantum critical polar metals, particularly in the superconducting state, have been predicted [37–42] by invoking a spin-orbit interaction mediated coupling between polar fluctuations and electrons in the vicinity of a polar quantum critical point (PQCP) with the appropriate interaction Hamiltonian

$$\hat{H}_{\text{int}} = \lambda \sum_{\mathbf{k}, \mathbf{q}} \sum_{s, s'} c_{\mathbf{k}+\mathbf{q}/2, s}^\dagger ((\mathbf{k} \times \hat{\boldsymbol{\sigma}}_{ss'}) \cdot \mathbf{P}_{\mathbf{q}}) c_{\mathbf{k}-\mathbf{q}/2, s'}, \quad (79)$$

where λ is the electron-phonon coupling constant, $c_{\mathbf{k}, s}^\dagger (c_{\mathbf{k}, s})$ is the electron creation (annihilation) operator with momentum \mathbf{k} , spin $s = \uparrow, \downarrow$, $\hat{\boldsymbol{\sigma}}$ is the Pauli matrix for spin and $\mathbf{P}_{\mathbf{q}}$ describes the polar order fluctuation field at a finite momentum \mathbf{q} . Here we note that the fluctuating phonon couples to the electronic spin current; since this coupling remains finite in the limit of $q \rightarrow 0$, it allows direct coupling to the critical mode, leading to a range of interesting phenomena emerging close to quantum criticality [37–42]. To date there is no consensus about the magnitude of this coupling in specific polar materials. Interestingly, very recent ab initio studies suggest a reasonable coupling of this type in doped strontium titanate [43], where it was previously not expected to be large [44]; this nearly polar metal has several unconventional

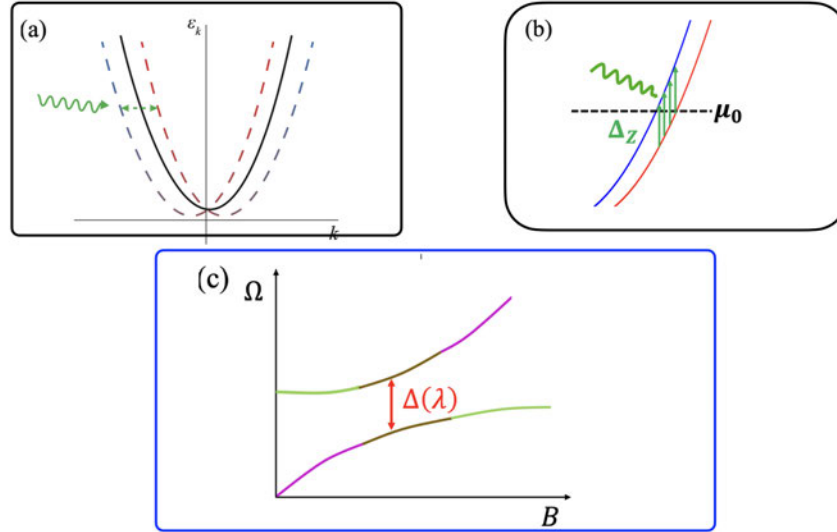


Fig. 9: Schematics of (a) the virtual spin-orbit assisted electron-phonon interaction, where the green (squiggly) line is the soft TO phonon, (b) the virtual spin-orbit mediated electron-TO phonon interaction in the presence of a magnetic field near the chemical potential μ_0 , (c) the avoided crossing of the soft polar and the electronic collective modes where Ω is frequency, B is magnetic field and Δ is a function of the Rashba-type electron-phonon coupling strength λ that can be extracted experimentally.

properties [34], possibly related to quantum critical polar fluctuations [45–47].

Is there any way to determine the strength of this type of coupling from experiment? The spin-assisted electron-phonon interaction influences the collective modes of a nearly polar metal in an applied magnetic field [48]. Here the soft polar phonon hybridizes with spin-flip electronic excitations of the Zeeman-split bands leading to an anticrossing in the spectra (see Figure 9). The associated splitting energies at the anticrossings can be used to determine the strength of the spin-orbit coupling mediated interactions between electrons and phonons in spectroscopic experiments, such as inelastic neutron scattering or IR spectroscopy, where estimates on known polar materials suggest that such measurements are currently experimentally accessible [48]; such measurements are in progress and will provide important constraints on theoretical descriptions of polar metals, particularly in their superconducting states where there are many mysteries [34, 40].

3.3 Multiband strongly correlated electronic phases

The Yukawa coupling of the order parameter (φ) to carriers

$$H_Y = \lambda \int d\mathbf{r} \varphi(\mathbf{r}) c^\dagger(\mathbf{r})c(\mathbf{r}) \quad (80)$$

is known to induce strong correlations for other types of quantum critical points, and so naturally we can ask whether it can also do so near a PQCP [25, 35]. As we will discuss in this section, a robust Yukawa coupling (80) to a soft polar mode can be generically realized in multiband systems even without spin-orbit coupling (SOC) leading to pronounced interaction effects at band crossings.

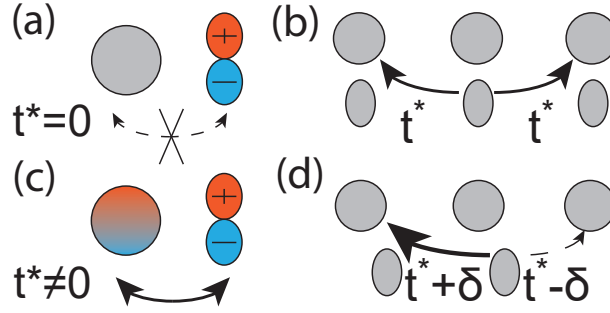


Fig. 10: Schematic of the coupling to the polar order parameter for two orbitals having (a,c) opposite and (b,d) same parity under inversion. (a) and (b) show the symmetric phase $\varphi^i = 0$, while (c) and (d) show the state for $\varphi^i \neq 0$. In both cases the interorbital hoppings change.

So how do the electrons here couple to an inversion symmetry-breaking field? What is wanted is a fermionic bilinear $\hat{O}^i(\mathbf{k})$ that breaks inversion symmetry (\mathcal{P}) leading to the coupling

$$H_{\text{coupling}} = \lambda \int d\mathbf{k} \varphi(\mathbf{k}) \hat{O}^i(\mathbf{k}), \quad (81)$$

first assuming time-reversal symmetry (\mathcal{T}). For a single conduction band without SOC, the only possible form of

$$\hat{O}(\mathbf{k}) = \hat{c}_{\mathbf{k}}^\dagger f_0(\mathbf{k}) \hat{c}_{\mathbf{k}} \quad \mathcal{P}, \mathcal{T} \rightarrow f_0. \quad (82)$$

Since both \mathcal{P} and \mathcal{T} require f_0 to be even, it is not possible for $\hat{O}(\mathbf{k})$ to break only inversion-symmetry. Yukawa polar coupling in a single-band model thus requires SOC.

By contrast, in a multiband system a Yukawa coupling can exist without SOC. In a two-band model \mathcal{T} is complex conjugation and \mathcal{P} acts in band space: $\mathcal{P} \sim \sigma_0$ for bands with the same parity or $\mathcal{P} \sim \sigma_3$ (up to a unitary transformation) in the opposite case. Writing a generic fermionic bilinear as $\hat{c}_{\mathbf{k}}^\dagger (f_0(\mathbf{k}) + \sum_{i=1}^3 f_i(\mathbf{k}) \sigma_i) \hat{c}_{\mathbf{k}}$, we find that the terms breaking inversion, but not time-reversal, symmetries are even in \mathbf{k} : $f_1(\mathbf{k})$ for $\mathcal{P} \sim \sigma_3$ or odd in \mathbf{k} : $f_2(\mathbf{k})$ for $\mathcal{P} \sim \sigma_0$. We can thus have the following Yukawa couplings to the polar mode at $\mathbf{q} \approx 0$

$$\begin{aligned} H_{\text{coupl}}^{(a)} &= \sum_{i,\mathbf{q},\mathbf{k}} f_a^i(\mathbf{k}) \varphi_{\mathbf{q}}^i c_{\mathbf{k}+\mathbf{q}/2}^\dagger \sigma_1 c_{\mathbf{k}-\mathbf{q}/2}, \quad \mathcal{P} \sim \sigma_3 \\ H_{\text{coupl}}^{(b)} &= \sum_{i,\mathbf{q},\mathbf{k}} f_b^i(\mathbf{k}) \varphi_{\mathbf{q}}^i c_{\mathbf{k}+\mathbf{q}/2}^\dagger \sigma_2 c_{\mathbf{k}-\mathbf{q}/2}, \quad \mathcal{P} \sim \sigma_0, \end{aligned} \quad (83)$$

where $f_{a(b)}^i(\mathbf{k})$ is even(odd) in \mathbf{k} , and the order parameter couples to an *interband* bilinear (Fig.11(a), inset). If we assume the bands to originate from two distinct orbitals, the physical mechanism of this Yukawa polar coupling can be illustrated (Fig. 10). If the orbitals have different parity (e.g. s and p) (Fig.10 (a)), they are mixed linearly by an inversion-breaking perturbation. This mixing is reflected in a nonzero hybridization between the resulting bands, forbidden in the symmetric phase (Fig.10 (a)). Due to the necessity of \mathbf{k} -dependence, the similar parity case (Fig.10 (b)) cannot be viewed as local. We illustrate it by a nearest-neighbor hopping between the orbitals (Fig.10 (b)); absence of inversion symmetry yields distinct left and right interorbital hoppings from a given site.

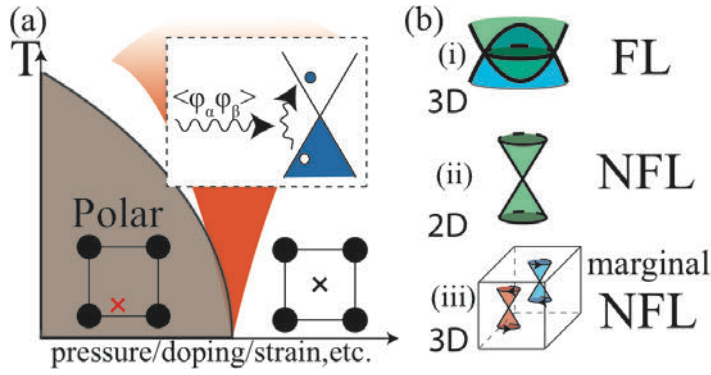


Fig. 11: (a) Schematic phase diagram of a polar metal with a critical region around the QCP. Inset illustrates that the critical fluctuations couple to an interband excitation. (b) Summary of the QCP behaviors near typical band crossing: (i) a 3D nodal line, (ii) a 2D nodal point, and (iii) 3D Weyl points. (N)FL is (non-)Fermi liquid, and in all cases the polar mode is strongly renormalized. Coulomb interactions introduce anisotropy for (i) and (ii), and gaps the longitudinal mode for (iii).

Can metals near polar quantum points host novel correlated phases? In order to drive unconventional metallic behavior already at weak coupling, the interband particle-hole excitations coupled to the critical mode with (83) need to be gapless. The best case scenario occurs when the two bands cross close to the Fermi energy, a situation that can be realized by carrier doping, where a low energy theory can be constructed. The critical behavior for three distinct cases (2D Dirac and 3D Weyl points, and 3D nodal lines) with and without interactions has been studied with and without Coulomb interactions. For all band crossing types, the critical polar mode is strongly renormalized and there is the emergence of non-Fermi liquid behavior for the two nodal point cases (Fig. 11). Details for the curious reader are available elsewhere along with experimental signatures for thermodynamic and transport properties [36].

The Rundown. In a nutshell, quantum critical polar metals provide settings to study exotic electron-phonon couplings due to the symmetry of the critical mode. Even in the absence of spin-orbit assisted interactions, nodal multiband metals provide promising platforms for novel metallic behaviors near polar quantum points. More specifically here we have discussed a generic mechanism for Yukawa-type coupling of the electronic density to the critical polar mode accessible even at weak coupling. We have identified novel interacting phases, including non-Fermi liquids, when band crossing are close to the Fermi level, with experimental signatures for generic types of band crossings [36]. As always these results prompt more questions; they include

- A number of polar materials with multiband electronic structures, including LiOsO_3 [49], MoTe_2 [50] and WTe_2 [51], have been recently discovered with many more predicted [32]. Can application of realistic pressures, external or chemical, drive these polar system to quantum criticality? How do spin-orbit effects, not considered here but present in several of these materials, compete with the Yukawa phases we have discussed here?
- Can new “flavors” of superconductivity emerge from the exotic metallic states we have discussed and, if so, what would be their key distinctive experimental signatures?

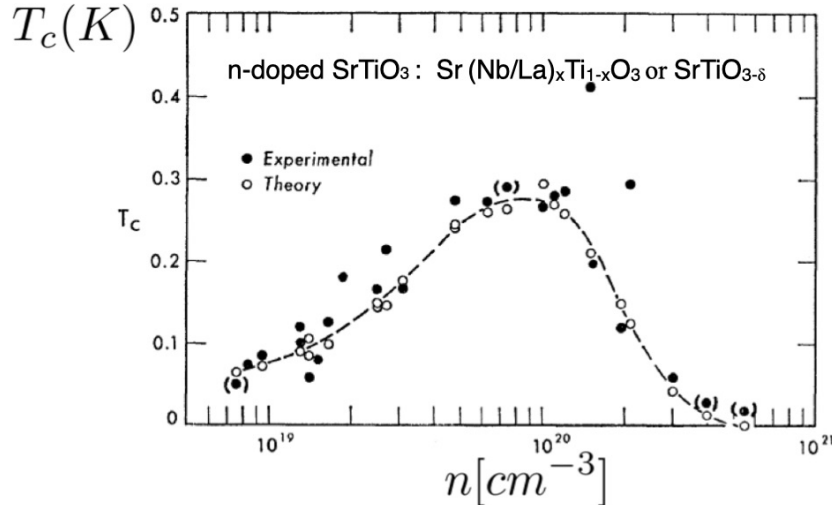


Fig. 12: The first study of the transition temperature as a function of carrier concentration for *n*-doped SrTiO₃ with good fit between the Cohen theory and experiment. Reprinted from [54] with permission from the American Physical Society.

4 Unconventional superconductivity (with only phonons!)

4.1 The challenge: anti-adiabatic and isotropic!

We have just seen that novel metallic states can occur near polar QCPs and we have even wondered whether such phases can lead to novel types of superconductivity. **A simpler question: can polar quantum criticality drive dilute (unconventional) superconductivity from a parent Fermi liquid state?** In conventional superconductors, electrons exploit the electron-phonon attraction to overcome the Coulomb repulsion by producing a highly retarded attraction that pairs electrons [52], a process that requires a large ratio between the Fermi and Debye energies $E_F/\omega_D \gg 1$. A challenge to this mechanism is posed by superconductivity in low carrier density metals near polar quantum critical points (PQCPs). Such materials, typified by *n*-doped SrTiO₃ (nSTO) [34], exhibit bulk superconductivity down to carrier densities of order 10^{19} cm^{-3} , where the relevant phonon frequency significantly exceeds the Fermi energy [34]. Proximity to the polar quantum critical point has been observed to enhance superconductivity in nSTO [53], suggesting that the underlying polar quantum criticality is a key driver to the pairing despite the decoupling of the critical polar modes from the electrons at low momenta [40,45,47]. Finally, despite this inversion of energy scales, experiments on nSTO indicate a conventional *s*-wave condensate, with a ratio of gap to transition temperature $2\Delta/T_c \approx 3.5$ in agreement with BCS theory and the normal state is a good Fermi liquid [34].

4.2 Historical context

Historically superconductivity in dilute nSTO was predicted based on an extension of conventional BCS theory to include multivalley phonons as a way to overcome Coulomb repulsion. The predicted transition temperature T_c versus doping, shown in Fig. 12, fit very well with experiment [54]. There was just one rub: band-structure calculations, performed after the original

prediction, indicated that nSTO has just one valley, so the theoretical premise of the prediction/confirmation by experiment needed reassessment and the mystery continues [34]. We note that in nSTO the enigmatic superconductivity emerges from a well-behaved Fermi liquid [34]. Over the years many theories have been developed to explain superconductivity in nSTO and other quantum critical polar metals using novel electron-phonon interactions with generalizations to include plasmons. More recently the importance of quantum criticality has been incorporated into theories with multiband effects and spin-orbit coupling; the curious reader is referred to an excellent recent review that surveys these different approaches [40].

4.3 Superconductivity with transverse phonons

Here we revisit superconductivity in quantum critical polar metals, particularly nSTO, guided by two key observations: first, that the strong ionic screening associated with the enhanced dielectric constant severely weakens the electronic Coulomb interaction (Fig. 13(a)); second, that in the absence of strong spin-orbit coupling the transverse optical phonon modes, decoupled from the electron charge, can be likened to dark matter, for like baryons in the cosmos, the electrons do not directly interact with the intense background of zero-point dipole fluctuations. Furthermore like dark matter, the presence of the TO modes is only revealed to the electrons via their stress-energy tensor. In particular, the electrons interact with the energy density of the TO phonons. We model this coupling by the Hamiltonian

$$H_{\text{En}} = g \int d^3x \rho_e(\mathbf{x}) (\vec{P}(\mathbf{x}))^2 \quad (84)$$

where $\rho_e(\mathbf{x}) = \psi^\dagger(\mathbf{x})\psi(\mathbf{x})$ is the electron density, $(\vec{P}(\mathbf{x}))^2$ is proportional to the energy density of the local polarization \vec{P} and g is a coupling constant with the dimensions of volume. Microscopically, this interaction can arise from the short-range effects of the Coulomb force within a unit cell of the material. The presence of an additional charge at the conduction electron site modifies the potential profile for the ions. A local increase in the electron density attracts the surrounding positively charged ions, reducing the distance between them. This causes the local “effective spring constant” of the phonons to rise in regions of high electron density. The natural units for this interaction are therefore atomic ones, i.e., unit cell volume, and should not be extremely different between different materials.

This coupling suppresses the zero-point fluctuations of the polarization in the vicinity of electrons, which in turn lowers the chemical potential of nearby electrons (Fig. 13(b)), creating an attractive potential well. To leading order, the resulting attractive potential is described by the virtual exchange of pairs of transverse optical phonons [47]: this approach is supported by other results:

- According to Equation (84), the presence of a finite electron density $n_e = \langle \rho_e(x) \rangle$ leads to a shift in the phonon frequency

$$\omega_T^2(n_e) = \omega_{T0}^2 + 2gn_e\varepsilon_0\Omega_0^2, \quad (85)$$

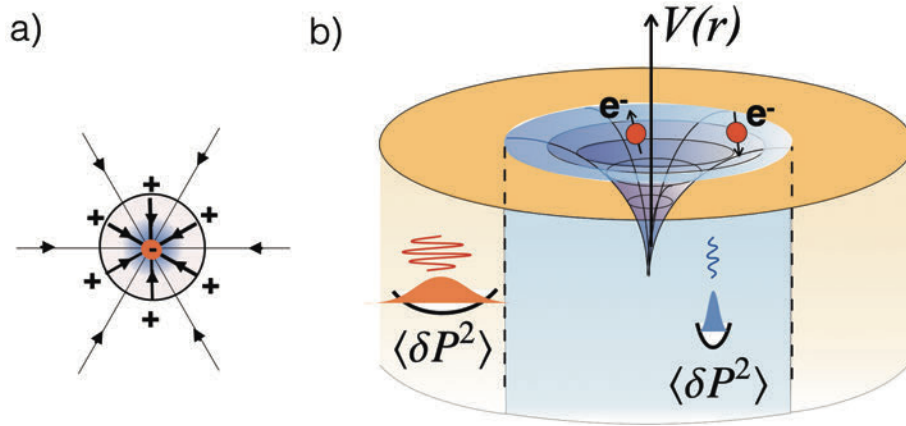


Fig. 13: Interactions between electrons in a quantum critical polar metal: (a) the electric lines of force around an electron are ionically screened, (b) the fluctuations of the phonon energy density around electrons (see Eq.(84)) create an attractive potential well.

which naturally explains the observed suppression of the polar state by charge doping in polar metals; neutron scattering measurements that probe the hardening of the polar mode with doping indicate that the charge density couples to the phonon energy rather than to its displacement [33, 55].

- Many quantum critical polar metals display “high-temperature” T^2 resistivity well above their Fermi temperatures [34], and a two-phonon exchange mechanism has been proposed to describe this anomalous transport [46].

Reviving an old idea [56, 57] and generalizing it to include polar quantum criticality, we now explore whether two-phonon processes can drive superconductivity in a quantum critical polar metal from a Fermi liquid state. [47, 58].

In this scenario, what is the interaction relevant for electron pairing?? Typically dilute systems require strong coupling approaches since the ratio of the Coulomb to the kinetic energy $r_s = 1/(k_F a_B) \gg 1$ since $k_F \propto n^{1/3}$. However in dilute quantum critical polar metals $a_B \propto \epsilon$ and thus is very large leading to $r_s \ll 1$; quantum critical polar metals then are weakly interacting and thus can be treated by considering perturbative effects. To lowest order, the virtual exchange of critical phonon pairs is the electron-electron interaction from two-phonon exchange. Close to the PQCP, the interaction relevant for electron pairing, averaged over the Fermi surface, is

$$\langle V(k-k') \rangle = \langle V(k_F, \theta) \rangle_\theta \sim -\frac{g^2}{c_s^3} \log \frac{\Omega_T}{\max(\omega_T, c_s k_F, E_f)} \quad (86)$$

where $\Omega_T = \max_{\vec{q}} \omega_T(\vec{q})$ cutoff and we see that large momenta contribute; ω_T is the soft (transverse) polar phonon. This interaction is dependent on carrier density since $k_F \propto n^{1/3}$ and $E_F \propto n^{2/3}$. At low densities close to the PQCP we have $E_F < c k_F$, so the interaction can be considered as instantaneous.

Can this interaction overcome Coulomb repulsion to lead to superconductivity? For carrier densities where $c_s k_F$ is the dominant energy scale, this attractive electron-electron interaction will indeed overcome the Coulomb repulsion leading to superconductivity. The attractive part of the effective electron coupling is

$$\lambda_{att} \sim k_F \left[\log \left(\frac{\Omega_T}{2c_s k_F} \right) + 1 \right] \quad (87)$$

that has the form $\lambda(x) = -x \log x + x$. Inclusion of Coulomb repulsion results in

$$\lambda \sim k_F \left(\left[\log \left(\frac{\Omega_T}{2c_s k_F} \right) + 1 \right] - \frac{C}{\epsilon_0} \right). \quad (88)$$

that leads to

$$T_c \propto E_F e^{-1/\lambda} \quad \frac{2\Delta}{T_c} = 3.5 \quad (89)$$

using a previously known approach [59]. The key take-home message here is that T_c has dome-like behavior as a function of the carrier density n_e and details of this approach are available elsewhere for a curious reader [47].

4.4 Comparison with experiment ... and homework!

Because filamentary superconductivity is suspected for very low carrier density superconducting n-doped SrTiO₃ (nSTO), detailed comparison here will be made to experiment for densities greater than $5 \cdot 10^{-18} \text{ cm}^{-3}$, corresponding to where $c_s k_F$ is the dominant energy scale and where bulk effects are observed [34]. As shown in Figure 14, the agreement between theory (solid line) and experiment (crosses) is reasonably good for a decade up to densities of roughly $5 \cdot 10^{-19} \text{ cm}^{-3}$, corresponding to its region of validity ($2c_s k_F > E_F$). It is to be noted that a better fit to the experimental data (crosses) for a larger density range is achieved by neglecting Coulomb interactions (dashed gray lines in Figure 14) but this is completely unjustified [47].

For densities higher than $5 \cdot 10^{-19} \text{ cm}^{-3}$, E_F is the dominant energy scale and dynamical aspects of the interaction cannot be ignored. At these densities, electronic as well as ionic contributions to the screening of the Coulomb interaction must be included, and we expect the Coulomb repulsion to increase as a function of frequency whereas the electron-electron attraction will behave in the opposite manner. We thus expect the overall interaction to change sign as a function of frequency, allowing for the enhancement of pairing by retardation effects [60]. However such a dynamical approach by itself does not lead to an attractive interaction in the dilute case; thus both energy fluctuations and dynamical screening, must be included to describe the full range of carrier concentrations where bulk superconductivity in n-doped SrTiO₃ is observed.

The Rundown. Typified by anti-adiabatic behavior and a “domed” T_c as function of carrier density, unconventional superconductivity (with only phonons!) has been observed in several low-density polar metals near polar quantum critical points, though there is still no consensus on the underlying mechanisms involved. Motivated by an approach that unifies different properties, here we have explored electron pairing mediated by energy fluctuations; it is already known to

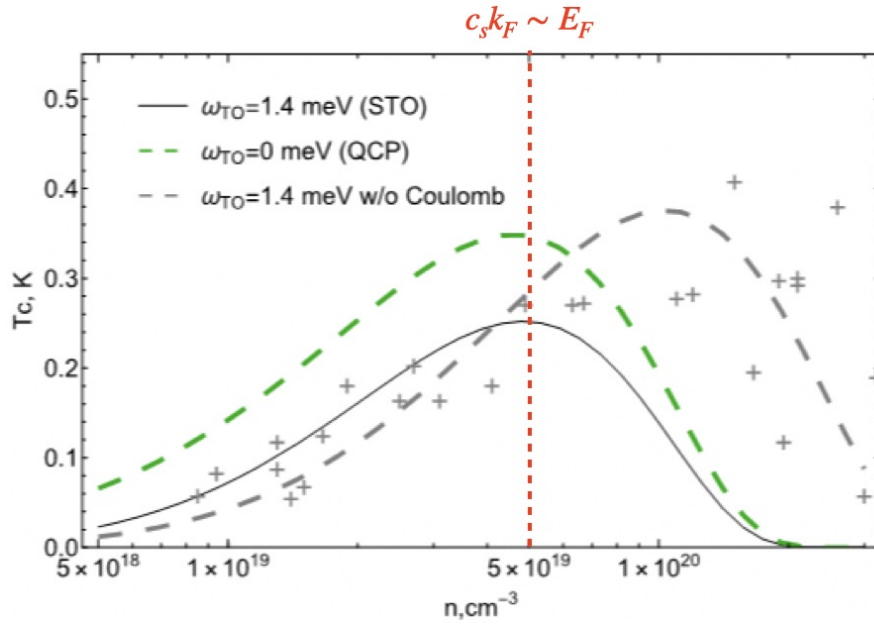


Fig. 14: The superconducting T_c for n -doped SrTiO_3 as a function of carrier concentration where the crosses and lines refer to experiment and theory respectively; the instantaneous approach taken ($c_S k_F$ is dominant energy-scale) is only valid up to $n \sim 5 \cdot 10^{-19} \text{ cm}^{-3}$, so for higher densities dynamical effects must be included.

describe the shift of the quantum critical point with doping [55] and anomalous normal state transport at high temperatures [46]. We find that this approach leads to a superconducting dome, $T_c(n_e)$, that is in good agreement with experiment at low doping. However for higher carrier densities E_F is the dominant energy scale in (86) and dynamical effects should be included. Yet signatures of the two-phonon mechanism including the soft phonon hardening and $\rho \propto T^2$ persist [33,34,55], suggesting that both energy fluctuations and dynamical screening contribute to the superconductivity in nSTO and in other quantum critical polar metals for a broad range of carrier concentrations.

Let us now step back and think more generally. Transverse modes are traditionally absent in theories of phonon-based superconductivity, as they do not couple to the charge density. However our discussion of doped quantum paraelectrics has revealed that superconductivity can be driven by multiple critical transverse phonons, a new channel for superconductivity in materials with large anharmonicity. The $3d$ electron pairing mediated by quantum energy fluctuations, an exchange of two critical transverse phonons at leading order, describes the dome-line structure of the superconducting phase diagram at low doping. In order to describe the observed superconducting behavior of the full range of carrier concentrations, this energy fluctuation pairing mechanism must be generalized dynamically, requiring the inclusion of longitudinal fluctuations. The resulting theory that includes both transverse and longitudinal phonons should be applicable well beyond the realm of quantum critical polar superconductors; it may be helpful to describe quantum materials with light electrons including magnesium diboride and the superconducting hydrides where significant nonlinear elasticity is present.

5 Summary and outlook

In these Lecture Notes, I have tried to convey my excitement and enthusiasm for the area of polar quantum criticality, emphasizing aspects that may not be part of the mainstream literature. We began by unpacking the title, discussing key concepts in quantum criticality, particularly phenomenological approaches towards determining measured low-temperature quantities. Next we presented polar materials, and we floated concerns about introducing these systems as research settings for quantum criticality which we subsequently addressed. Experimentally many compressible polar materials are found to have discontinuous finite-temperature transitions coexisting with quantum critical behavior, and we discussed a theoretical basis for this phenomenon. Because the approach here is subtle and not that well known, we have spent some effort outlining the arguments carefully. The quest for novel metallicity and unconventional superconductivity is a key motivation for research activity on quantum criticality, so next we show that both occur near polar quantum critical points. Furthermore symmetry demands that nontraditional electron-phonon interactions can be explored in this setting with implications beyond the original realm.

More generally we recall that polar phenomena are classical examples of emergent behavior in solids that have been important for many technological applications. Recently polar phenomena have been observed in several correlated materials where quantum effects dominate, including frustrated magnets, Mott insulators, non-Fermi liquid and Moire superlattices and there is much to be done towards understanding and harnessing the rich polar properties of quantum materials. The presence of polar behavior in these strongly correlated quantum materials provides opportunities to

- Identify and characterize new electrically active states of quantum matter including electron dipole liquids and quantum critical multiferroics
- Probe quantum matter using electric field-based tools
- Develop quantum states of matter that can be tuned and controlled by electric fields towards practical quantum device applications

and the study of these fascinating materials at cryogenic temperatures near quantum criticality is a way to focus on their predominantly quantum behaviors. In addition, the neighborhood of a polar quantum critical point is a good setting for these explorations since it is a scale-free zone where the Coulomb repulsion is significantly weakened. Possible research directions for the future include:

- Mixed parity states in polar superconductors. Polar superconductors are by definition non-centrosymmetric and thus defy standard classification schemes; exotic properties like unusual surface states and magnetoelectric effects could occur.
- The relation between polarization and band topology. Because the Coulomb interaction is weak near a polar quantum critical point, this could be an excellent setting to study polarization textures.

- Dynamical quantum criticality has been studied in synthetic quantum systems. Since polar materials have soft optical modes, they are good settings for photoinduced classical transitions [61]. What experimental signatures would be expected at a dynamical quantum critical point?
- Interfacial and stacked ferroelectricity has been recently demonstrated in layered van der Waals structures that depend sensitively on the stacking configurations of the layers involved [62], and I would be remiss if I did not mention this fascinating development. Because the nature of these polar system is so different than that which we have discussed so far, there are bound to be fascinating new phenomena here to study, particularly related to the electrooptical properties of these heterostructures.

The list can of course go on and on. I hope that I have given you a flavor for polar quantum criticality with its many challenges and its many opportunities. Please come and join the fun!

Acknowledgements

This work is result of many wonderful collaborations with P. Coleman, M.A. Continentino, A. Kumar, G.G. Lonzarich, L. Palova, S.E. Rowley, J.F. Scott, P.A. Volkov and of course many stimulating discussion with countless colleagues. I am grateful to them all for sharing their knowledge and their insights with me in this fascinating area and more. I have tried to provide references whenever possible for further reading/clarification; due to space restrictions naturally the bibliography is not exhaustive, and I apologize in advance to colleagues whose research may be inadvertently not represented. This work was performed in part at the Aspen Center for Physics, which is supported by National Science Foundation grant PHY-2210452.

References

- [1] S. Sachdev: *Quantum Phase Transitions* (Cambridge University Press, 1999)
- [2] P. Coleman and A. Schofield, *Nature* **433**, 226 (2005)
- [3] S. Sachdev, *Nat. Phys.* **4**, 173 (2008)
- [4] M.A. Continentino: *Quantum Scaling in Many-Body Systems* (World Scientific, Singapore, 2001)
- [5] M. Vojta, *Rep. Prog. Phys.* **66**, 2069 (2003)
- [6] P. Chandra, G. Lonzarich, S. Rowley, and J. Scott, *Rep. Prog. Phys.* **80**, 112502 (2017)
- [7] L. Palova, P. Chandra, and P. Coleman, *Phys. Rev. B* **79**, 075101 (2009)
- [8] L. Landau and E. Lifshitz: *Statistical Physics* (Pergamon Press, Oxford, 1980)
- [9] P. Chandra and P. Littlewood, pp. 69–115 in [63]
- [10] S. Rowley, L. Spalek, R. Smith, M. Dean, M. Itoh, J. Scott, G. Lonzarich, and S. Saxena, *Nat. Phys.* **10**, 367 (2014)
- [11] E. Fatuzzo and W. Merz: *Ferroelectricity* (North-Holland, Amsterdam, 1967)
- [12] M. Lines and A. Glass: *Principles and Applications of Ferroelectrics and Related Materials* (Clarendon Press, Oxford, 1977)
- [13] F. Jona and G. Shirane: *Ferroelectric Crystals* (Dover Publications, New York, 1993)
- [14] B. Strukov and A. Levanyuk: *Ferroelectric Phenomena in Crystals: Physical Foundations* (Springer, Heidelberg, 1998)
- [15] K.M. Rabe, M. Dawber, C. Lichtensteiger, C.H. Ahn, and J.M. Triscone, pp. 1–29 in [63]
- [16] A. Larkin and D. Khmel'nitskii, *Sov. Phys. JETP* **29**, 11231128 (1969)
- [17] P. Chandra, *Nat. Phys.* **19**, 1525 (2023)
- [18] G. Ahlers, A. Kornbilit, and H. Guggenheim, *Phys. Rev. Lett.* **34**, 1227 (1975)
- [19] E. Sandvold and E. Courtens, *Phys. Rev. B* **27**, 5660 (1983)
- [20] B. Chakrabati, A. Dutta, and P. Sen: *Quantum Ising Phases and Transitions in Transverse Ising Models* (Springer, Heidelberg, 1996)
- [21] O. Kvyatkovskii, *Phys. Solid State* **43**, 1401 (2001)
- [22] A. Rechester, *Sov. Phys. JETP* **33**, 423 (1971)

- [23] R. Roussev and A. Millis, *Phys. Rev. B* **67**, 014105 (2003)
- [24] J. Cardy: *Scaling and renormalization in statistical physics*, Vol. 5 (Cambridge University Press, 1996)
- [25] M. Brando, D. Belitz, F.M. Grosche, and T.R. Kirkpatrick, *Rev. Mod. Phys.* **88**, 025006 (2016)
- [26] A. Larkin and S. Pikin, *Sov. Phys. JETP* **29**, 891 (1969)
- [27] P. Chandra, P. Coleman, M.A. Continentino, and G. Lonzarich, *Phys. Rev. Res.* **2**, 043440 (2020)
- [28] P.P. Edwards and M.J. Sienko, *Phys. Rev. B* **17**, 2575 (1978)
- [29] X. Lin, Z. Zhu, B. Fauqué, and K. Behnia, *Phys. Rev. X* **3**, 021002 (2013)
- [30] P.W. Anderson and E.I. Blount, *Phys. Rev. Lett.* **14**, 217 (1965)
- [31] N. Benedek and T. Birol, *J. Mat. Chem. C* **4**, 4000 (2016)
- [32] S. Bhowal and N.A. Spaldin, *Annu. Rev. Mat. Res.* **53**, 53 (2023)
- [33] C.W. Rischau, X. Lin, C.P. Grams, D. Finck, S. Harms, J. Engelmayer, T. Lorenz, Y. Gallais, B. Fauque, J. Hemberger, and K. Behnia, *Nat. Phys.* **13**, 643 (2017)
- [34] C. Collignon, X. Lin, C.W. Rischau, B. Fauque, and K. Behnia, *Annu. Rev. Condens. Matter Phys.* **10**, 25 (2019)
- [35] A. Abanov, A.V. Chubukov, and J. Schmalian, *Adv. Phys.* **52**, 119 (2003)
- [36] P.A. Volkov and P. Chandra, *Phys. Rev. Lett.* **124**, 237601 (2020)
- [37] V. Kozii and L. Fu, *Phys. Rev. Lett.* **115**, 207002 (2015)
- [38] J. Ruhman, V. Kozii, and L. Fu, *Phys. Rev. Lett.* **118**, 227001 (2017)
- [39] S. Kanasugi and Y. Yanase, *Phys. Rev. B* **100**, 094504 (2019)
- [40] M.N. Gastiasoro, J. Ruhman, and R.M. Fernandes, *Ann. Phys.* **417**, 168107 (2020)
- [41] M.N. Gastiasoro, M.E. Temperini, P. Barone, and J. Lorenzana, *Phys. Rev. Res.* **5**, 023177 (2023)
- [42] A. Klein, V. Kozii, J. Ruhman, and R.M. Fernandes, *Phys. Rev. B* **107**, 165110 (2023)
- [43] M.N. Gastiasoro, M.E. Temperini, P. Barone, and J. Lorenzana, *Phys. Rev. B* **105**, 224503 (2022)
- [44] J. Ruhman and P.A. Lee, *Phys. Rev. B* **100**, 226501 (2019)

- [45] J.M. Edge, Y. Kedem, U. Aschauer, N.A. Spaldin, and A.V. Balatsky, *Phys. Rev. Lett.* **115**, 247002 (2015)
- [46] A. Kumar, V.I. Yudson, and D.L. Maslov, *Phys. Rev. Lett.* **126**, 076601 (2021)
- [47] P. Volkov, P. Chandra, and P. Coleman, *Nat. Commun.* **13**, 4599 (2021)
- [48] A. Kumar, P. Chandra, and P.A. Volkov, *Phys. Rev. B* **105**, 125142 (2022)
- [49] Y. Shi, Y. Guo, X. Wang, A.J. Princep, D. Khalyavin, P. Manuel, Y. Michiue, A. Sato, K. Tsuda, S. Yu, M. Arai, Y. Shirako, M. Akaogi, N. Wang, K. Yamaura, and A.T. Boothroyd, *Nat. Mat.* **12**, 1024 (2013)
- [50] J. Jiang, Z. Liu, Y. Sun, H. Yang, C. Rajamathi, Y. Qi, L. Yang, C. Chen, H. Peng, C. Hwang et al., *Nat. Commun.* **8**, 13973 (2017)
- [51] Z. Fei, W. Zhao, T.A. Palomaki, B. Sun, M.K. Miller, Z. Zhao, J. Yan, X. Xu, and D.H. Cobden, *Nature* **560**, 336 (2018)
- [52] P. Coleman: *Introduction to Many-Body Physics* (Cambridge University Press, 2015)
- [53] M.J. Coak, C.R. Haines, C. Liu, S.E. Rowley, G.G. Lonzarich, and S.S. Saxena, *Proc. Nat. Acad. Sci. U.S.A.* **117**, 12707 (2020)
- [54] C.S. Koonce, M.L. Cohen, J.F. Schooley, W.R. Hosler, and E.R. Pfeiffer, *Phys. Rev.* **163**, 380 (1967)
- [55] D. Bäuerle, D. Wagner, M. Wöhlecke, B. Dorner, and H. Kraxenberger, *Z. Phys. B Condens. Matter* **38**, 335 (1980)
- [56] K.L. Ngai, *Phys. Rev. Lett.* **32**, 215 (1974)
- [57] D. van der Marel, F. Barantani, and C.W. Rischau, *Phys. Rev. Res.* **1**, 013003 (2019)
- [58] D.E. Kiselov and M.V. Feigel'man, *Phys. Rev. B* **104**, L220506 (2021)
- [59] L.P. Gor'kov, *Phys. Rev. B* **93**, 054517 (2016)
- [60] D. Pimenov and A.V. Chubukov, *Ann. Phys.* **447**, 169049 (2022)
- [61] Z. Zhuang, A. Chakraborty, P. Chandra, P. Coleman, and P.A. Volkov, *Phys. Rev. B* **107**, 224307 (2023)
- [62] E.Y. Tsymbal, *Science* **372**, 1389 (2021)
- [63] K. Rabe, C. Ahn, and J. Triscone (Eds.): *Physics of Ferroelectrics: A Modern Perspective* (Springer, Heidelberg, 2007)